Tectonics

RESEARCH ARTICLE
10.1029/2020TC006063

Microcontinents and Continental Fragments Associated With Subduction Systems

J. M. van den Broek[1] and C. Gaina[1]

[1]The Centre for Earth Evolution and Dynamics (CEED), Department of Geosciences, University of Oslo, Oslo, Norway

Abstract Microcontinents and continental fragments are small pieces of continental crust that are surrounded by oceanic lithosphere. Although classically associated with passive margin formation, here we present several preserved microcontinents and continental fragments associated with subduction systems. They are located in the Coral Sea, South China Sea, central Mediterranean and Scotia Sea regions, and a "proto-microcontinent," in the Gulf of California. Reviewing the tectonic history of each region and interpreting a variety of geophysical data allows us to identify parameters controlling the formation of microcontinents and continental fragments in subduction settings. All these tectonic blocks experienced long, complex tectonic histories with an important role for developing inherited structures. They tend to form in back-arc locations and separate from their parent continent by oblique or rotational kinematics. The separated continental pieces and associated marginal basins are generally small and their formation is quick (<50 Myr). Microcontinents and continental fragments formed close to large continental masses tend to form faster than those created in systems bordered by large oceanic plates. A common triggering mechanism for their formation is difficult to identify, but seems to be linked with rapid changes of complex subduction dynamics. The young ages of all contemporary pieces found in situ suggest that microcontinents and continental fragments in these settings are short lived. Although presently the amount of in-situ subduction-related microcontinents is meager (an area of 0.56% and 0.28% of global, non-cratonic, continental crustal area and crustal volume, respectively), through time microcontinents contributed to terrane amalgamation and larger continent formation.

Key Points:
- Microcontinents can form in association with convergent plate boundaries which experienced long and complex histories
- Formation often requires oblique or rotational kinematics as well as the presence of inherited structures in the continental crust
- Changes in slab dynamics is a potential mechanism that drives microcontinent formation in convergent settings

Supporting Information:
- Supporting Information S1
- Table S1

Correspondence to:
J. M. van den Broek,
j.v.d.broek@geo.uio.no

Citation:
van den Broek, J. M., & Gaina, C. (2020). Microcontinents and continental fragments associated with subduction systems. *Tectonics*, *39*, e2020TC006063. https://doi.org/10.1029/2020TC006063

Received 6 JAN 2020
Accepted 23 JUN 2020
Accepted article online 29 JUN 2020

1. Introduction

In the geological record, continental breakup and subsequent seafloor spreading sometimes resulted in smaller blocks being sliced and carried away from the margins of the parent continent. Changes in plate boundaries and other tectonic events moved these continental blocks back to larger continental masses and their continuously changing margins. The evolution of microcontinents is therefore an important mechanism for redistributing continental lithosphere and more information about it could shed light on various processes that affected continental margins through time. In addition, together with other scattered bathymetric features in the oceans, microcontinents played a meaningful role in paleogeography, paleo-ocean circulation, and biogeography.

Microcontinents and continental fragment formation has classically been associated with passive margin formation and accompanying divergent tectonic settings (e.g., Molnar et al., 2018; Müller et al., 2001; Nemčok et al., 2016; Péron-Pinvidic & Manatschal, 2010). However, several contemporary microcontinents and continental fragments formed in (association with) active continental margins. We aim to document these microcontinents and continental fragments and place their formation and evolution in a larger plate tectonic context. In doing so, we highlight the diversity and complexity of active continental margins and shed additional light on their evolution.

A microcontinent is defined as a piece of continental crust which has been horizontally displaced with respect to a continent, usually situated close by; it is surrounded by oceanic crust, and is smaller than the nearby/parent continent or than the smallest continent (Scrutton, 1976). Classic examples include the Jan-Mayen microcontinent in the north-east Atlantic Ocean (Gaina et al., 2009; Peron-Pinvidic et al., 2012a, 2012b) and the Seychelles in the Indian Ocean (Gaina et al., 2013; Ganerød et al., 2011; Torsvik et al., 2013). Continental fragments are defined similarly to microcontinents, with the exception that the complete separation from the parent continent did not occur (Lister et al., 1986). Examples include the Rockall and Porcupine Banks and the Galicia Bank, both in the North Atlantic (Péron-Pinvidic & Manatschal, 2010).

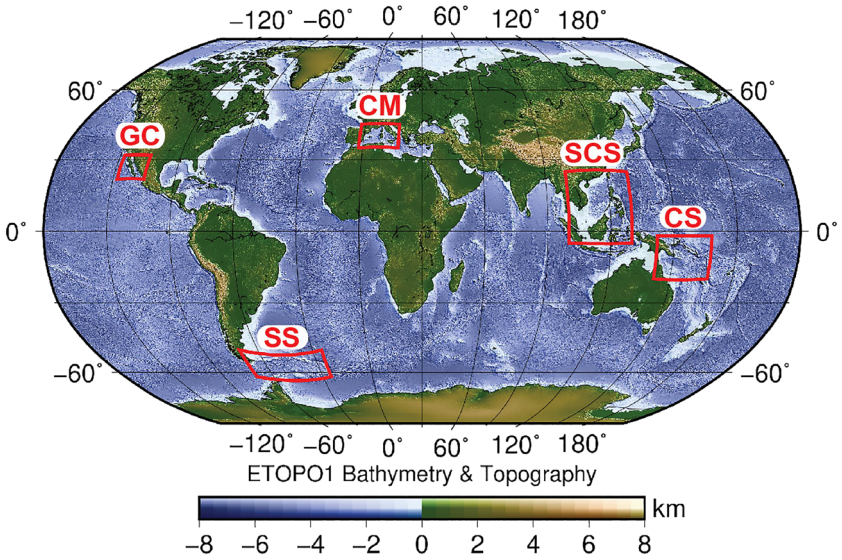

Figure 1. Global map with locations of the various regions studied in this work. CS = Coral Sea; SCS = South China Sea; CM = Central Mediterranean Sea; SS = Scotia Sea; GC = Gulf of California.

Various mechanisms have been proposed to explain the formation of the microcontinents and continental fragments mentioned above. One group of studies proposes microcontinent formation due to plate boundary relocations (ridge jumps) assisted by mantle heterogeneities (Abera et al., 2016; Müller et al., 2001). Other authors emphasize the role of inherited tectonic structures and the need for a strike-slip, or a rotational component in the breakup processes resulting in the isolation of a small fragment of continental crust (Molnar et al., 2018; Nemčok et al., 2016; Péron-Pinvidic & Manatschal, 2010; van den Broek et al., 2020).

An overview of continental active margins reveals the existence of small continental blocks situated in their proximity. The various continental pieces bordering the Coral Sea, NE of Australia (Gaina et al., 1999; Taylor & Falvey, 1977), the Reed and Macclesfield Banks in the South China Sea (Cullen et al., 2010; Pichot et al., 2014), the Corsica-Sardinia block in the Central Mediterranean (Advokaat et al., 2014; Faccenna et al., 2001), and various fragments in the Scotia Sea (Carter et al., 2014; Trouw et al., 1997) (Figure 1) all formed close to active continental margins and related subduction systems. In addition, rifting and spreading in the Gulf of California is separating the Baja California microplate from the North-American continent (Sutherland et al., 2012; Umhoefer, 2011), a process connected to the subduction of the Farallon plate under the North American plate.

The formation of microcontinents and continental fragments formed in convergent and/or subduction systems is an overlooked aspect of active margin evolution. To address this deficiency, we present a global catalogue of microcontinents and continental fragments associated to convergent margins. First, we review the overall tectonic setting and history of these microcontinents. Second, we reevaluate their present-day structure based on available geological and geophysical data. By studying patterns in their rifted margin morphology, we search for clues revealing potential mechanisms and/or parameters that controlled their formation. We then attempt to place microcontinent formation in subduction systems into a larger geodynamic context and asses its influence on global, non-cratonic, continental crust evolution.

For simplicity we group microcontinents and continental fragments associated with subduction and refer to them as microcontinents for the remainder of this paper. We define “proto-microcontinents” as pieces of continental lithosphere that are likely to (partially) separate from their parent continents in the future.

2. A Review of the Tectonic History of Microcontinents and Continental Fragments Associated With Subduction

We investigate microcontinents in regions affected by subduction in the following locations: (1) the Coral Sea; (2) the South China Sea; (3) the central Mediterranean Sea; (4) the Scotia Sea; and (5) the Gulf of

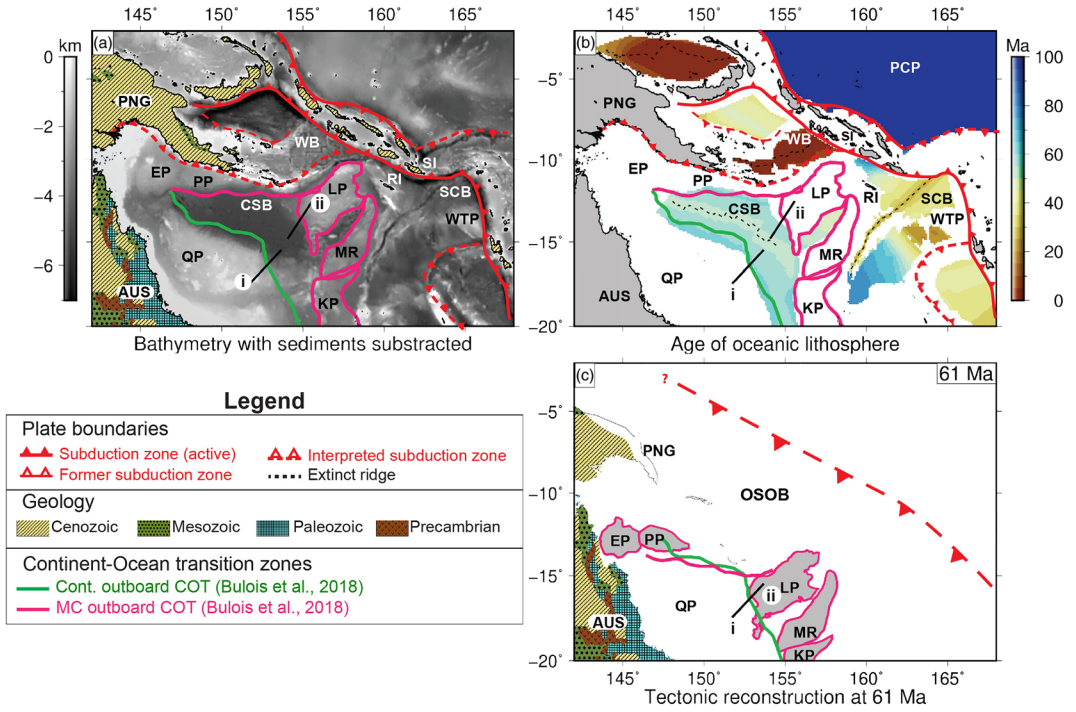

Figure 2. Geological models and bathymetric observations for the Coral Sea. (a) Bathymetry with sediments subtracted (no backstripping) and onshore geology. (b) Oceanic age grid of the various basins in the Coral Sea region. (c) Tentative tectonic reconstruction to the pre-Coral Sea breakup configuration. MC = microcontinent; LP = Louisiade Plateau; MR = Mellish Rise; KP = Kenn Plateau; WTP = West Torres Plateau; SCB = Santa Cruz Basin; RI = Rennel Island; WB = Woodlark Basin; PP = Papuan Plateau; EP = Eastern Plateau; PNG = Papua New Guinea; AUS = Australia; QP = Queensland Plateau; CSB = Coral Sea Basin; PCP = Pacific Plate; OSOB = Owen Stanley Oceanic Basin.

California (Figure 1). In the following we will review the tectonic evolution of each region with a focus on the relevant oceanic basins and the microcontinent(s).

In order to highlight the morphology of continental margins, we create a "no-sediment" bathymetry by subtracting the total sediment thickness estimation from the global bathymetric grid. Note that we do not preform backstripping, but simply remove the sediment thickness without compensating for depth adjustments. For bathymetry we use the ETOPO1 global relief model (Amante & Eakins, 2009). Sediment thickness in the Mediterranean region is from the EPcrust model (Molinari & Morelli, 2011), while for all other regions we utilize the GlobSed model from Straume et al. (2019). First-order onshore geological provinces from the third edition of the World Geological Map (Bouysse, 2014) are shown together with the offshore "no-sediment bathymetry" maps and on tectonic reconstruction maps in order to provide basic information about on-shore geology.

Kinematic reconstructions and oceanic age grids provide insight into the tectonic evolution of a region. Interpreted ages of oceanic crust are provided by the global oceanic age grid from Müller et al. (2008), while the location of spreading ridges are either reinterpreted for this study or taken from Müller et al. (2016). Tectonic reconstructions are produced with the open source software GPlates (http://www.gplates.org). The pre-breakup configurations and present-day microcontinent locations, together with the age of surrounding oceanic lithosphere (age grids), are presented in Figures 2–6. Additional kinematic reconstructions, mainly documenting plate boundary relocations that led to complete isolation of the microcontinents, are in the supporting information. Reconstructions for the Mediterranean region are from Advokaat et al. (2014) and van Hinsbergen et al. (2014). The pre-breakup reconstruction of the Coral Sea was created using the model of Seton et al. (2016), which is based on Gaina et al. (1999). Reconstruction parameters for the Scotia Sea are from Eagles and Jokat (2014). Both the South China Sea and the Gulf of California where reconstructed according to Matthews et al. (2016).

10.1029/2020TC006063

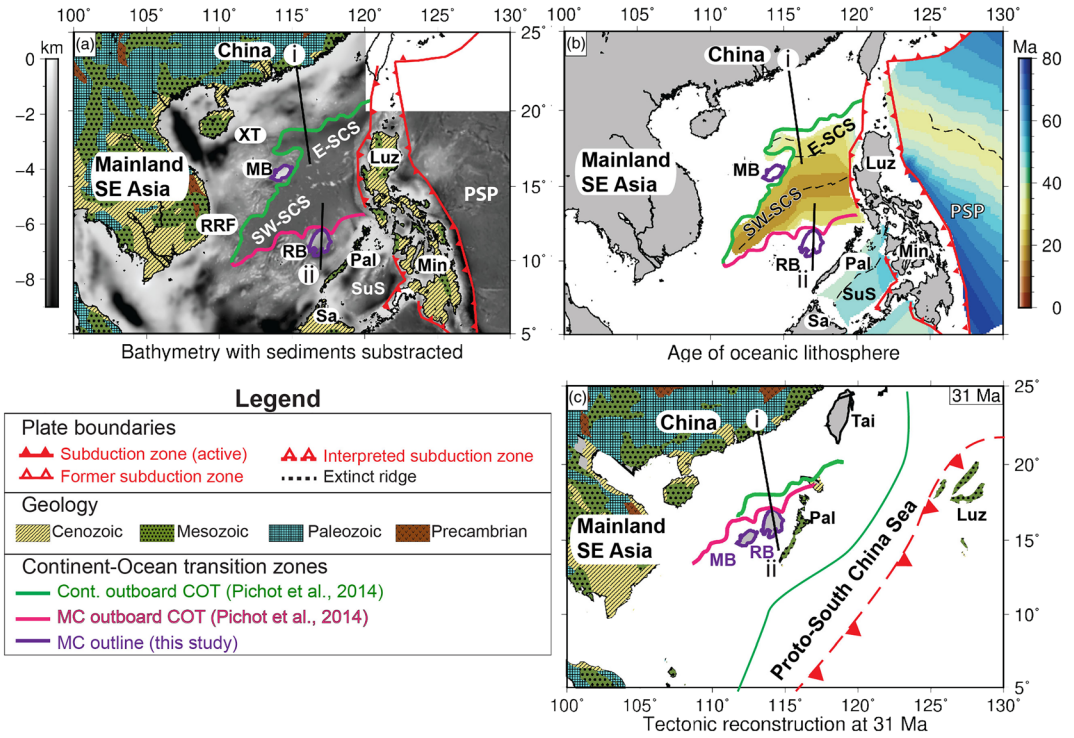

Figure 3. Geological models and bathymetric observations for the South China Sea. (a) Bathymetry with sediments subtracted (no backstripping) and onshore geology. (b) Oceanic age grid of the various basins in the South China Sea region. (c) Tentative tectonic reconstruction of the pre-breakup configuration of the South China Sea. XT = Xisha Through; MB = Macclesfield Bank; RB = Reed Bank; RRF = Red River Fault; SW-SCS = South West subbasin; E-SCS = Eastern subbasin; Luz = Luzon; PSP = Philippine Sea Plate; Min = Mindoro; Pal = Palawan; SuS = Sulawesi Sea; Tai = Taiwan.

2.1. The Coral Sea

The SW Pacific and the neighboring northeast margin of Australia are complex regions which have been shaped in the Cenozoic by various subduction episodes that resulted from changes in relative plate motions of the Australian and Pacific plates (Figure 2). The eastern margin of Australia/Gondwanaland was a long-lived convergent margin since at least the Cambrian (Glen, 2005) up until mid-Cretaceous times (Laird & Bradshaw, 2004). During this long-lived convergent margin setting, the NE Australian region experienced two rifting phases as recorded in the present-day sedimentary record (Bulois et al., 2018). The first rifting stage occurred in the Triassic and may have exploited crustal scale heterogeneities already present on the edge of the Australian craton (Bulois et al., 2018; Van Wyck & Williams, 2002). A subsequent rifting episode from the Jurassic to Lower Cretaceous exploited and reactivated these structures (Bulois et al., 2018). During this extension episode, new rift basins were created and this extended margin was considered to be the southern margin of the postulated "Owen Stanley Oceanic Basin" (Figure 2c) (Bulois et al., 2018). The existence of an older oceanic basin NE of Australia is inferred from the presence of supra-subduction zone ophiolites and ultramafic strata accreted in the Papuan fold and thrust belts (Bulois et al., 2018; Lus et al., 2004; Webb et al., 2014). This basin was supposedly formed as a back-arc basin due to a retreating Pacific slab.

The subduction configuration of the Pacific plate north and northeast of Australia probably changed around mid-Cretaceous time (Laird & Bradshaw, 2004), but the exact architecture of this region is difficult to reconstruct as subsequent tectonic episodes have overprinted its Cretaceous fabric (i.e., Seton et al., 2016). However, available geological evidence combined with plate circuit modeling suggests that west-dipping subduction continued from late Cretaceous to early Cenozoic, albeit at a slower pace. Associated back-arc basin opening occurred from the mid-upper Cretaceous to the early Eocene (Matthews et al., 2015). This last rifting episode of NE Australian margin in the upper Cretaceous ended with continental breakup and seafloor spreading along an axis that cross-cut the trends of the previous two rift systems. Note that the

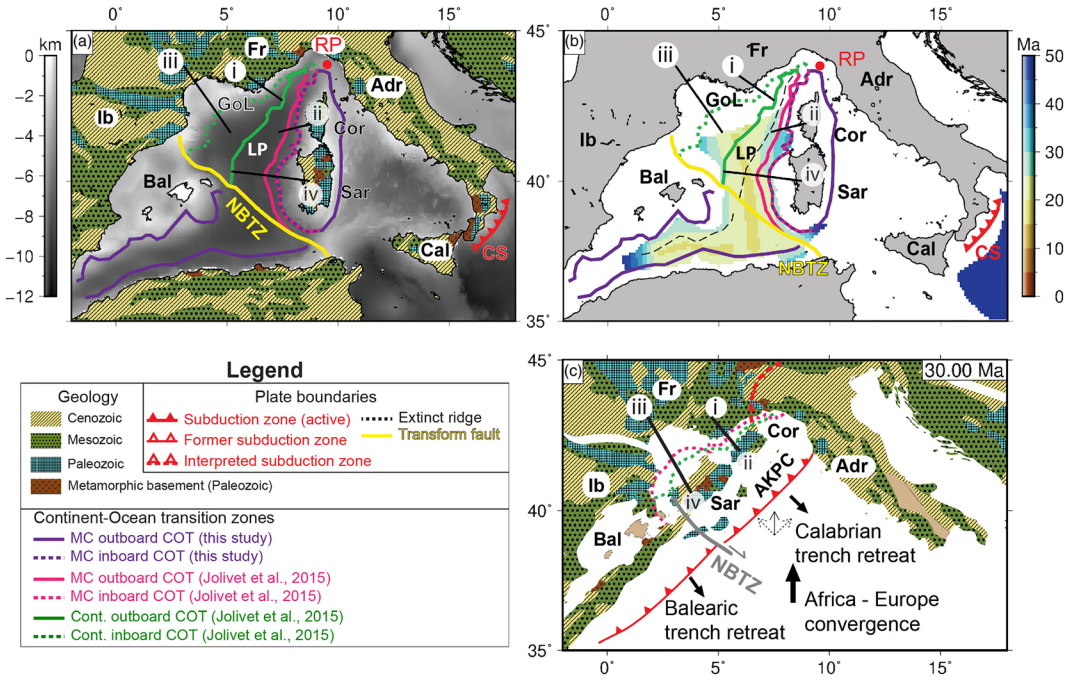

Figure 4. Geological models and bathymetric observations for the Central Mediterranean region. (a) Bathymetry with sediments subtracted (no backstripping) and onshore geology. (b) Oceanic age grid of the various basins in the Central Mediterranean. Note that this age grid is incorrect. (c) Tectonic reconstruction of the pre-breakup situation of the Central Mediterranean. Ib = Iberian Peninsula; GoL = Gulf of Lyon; Fr = France; Adr = Adria; CS = Calabrian Subduction Zone; Cal = Calabria; Cor = Corsica; Sar = Sardinnia; NBTZ = North Balearic Transfer Zone; RP = Rotation pole of the Liguro-Provençal basin; Bal = Balearic Islands; AKPC = AlKaPeCa terrane.

opening of the Coral Sea may have been associated to either NE subduction of the Australian plate under the Pacific plate (i.e., Whattam et al., 2008), or a SW subduction of the Pacific plate under the Australian plate. Geological evidences favor the first scenario, whereas slab remnants in the mantle can be invoked by both hypotheses (see section 3 and supporting information). Oceanic accretion in the Coral Sea started in the middle Paleocene and lasted until early Eocene (Figure 2b) (Gaina et al., 1999; Weissel & Watts, 1979).

Opening of the Coral Sea detached the Kenn, Louisiade and Papuan plateaus, and the Melish Rise from the NE Australian margin (Figure 2). The Eastern Plateau is still attached to the NE Australian margin via extended crust (Figure 2b). Cessation of Coral Sea seafloor spreading around 52 Ma has been attributed to changes in absolute plate motion direction (Eagles et al., 2004; Matthews et al., 2015; Schellart et al., 2006), or to the influence of subduction north and east of the basin along the Papuan-Rennel-New Caledonian trench system (Gaina et al., 1999). Subsequent subduction and back-arc basin formation resumed northeast of Coral Sea (Figure 2) (Matthews et al., 2015; Seton et al., 2016), and closure and accretion of oceanic (back-arc) basins onto Papua New Guinea occurred to the northwest (Lus et al., 2004).

2.2. The South China Sea

Southeast Asia is a complex amalgamation of terranes, continental fragments, island arcs, and associated marginal and back-arc basins (Figure 3) resulted from the interaction of the Pacific, Eurasian, and Australian plates (Ding et al., 2016; Wu et al., 2016; Zahirovic et al., 2014). Several authors proposed a north-west dipping, Andean type, subduction of the Paleo-Pacific plate below mainland SE Asia from the Middle Jurassic to Middle/late Cretaceous or early Eocene (Figure 3c) (Hall & Breitfeld, 2017; Taylor & Hayes, 1983; Zahirovic et al., 2014). This convergence potentially accreted various pieces of continental and island arc material to the margin (Breitfeld et al., 2017; Hennig et al., 2017; Pubellier et al., 2003). Around Paleocene times, roll back of the Paleo-Pacific plate resulted in the separation of the south Palawan block from the south Chinese paleo margin and the formation of the so called Proto South China Sea (Zahirovic et al., 2014). The subsequent Cenozoic evolution of the region is controversial.

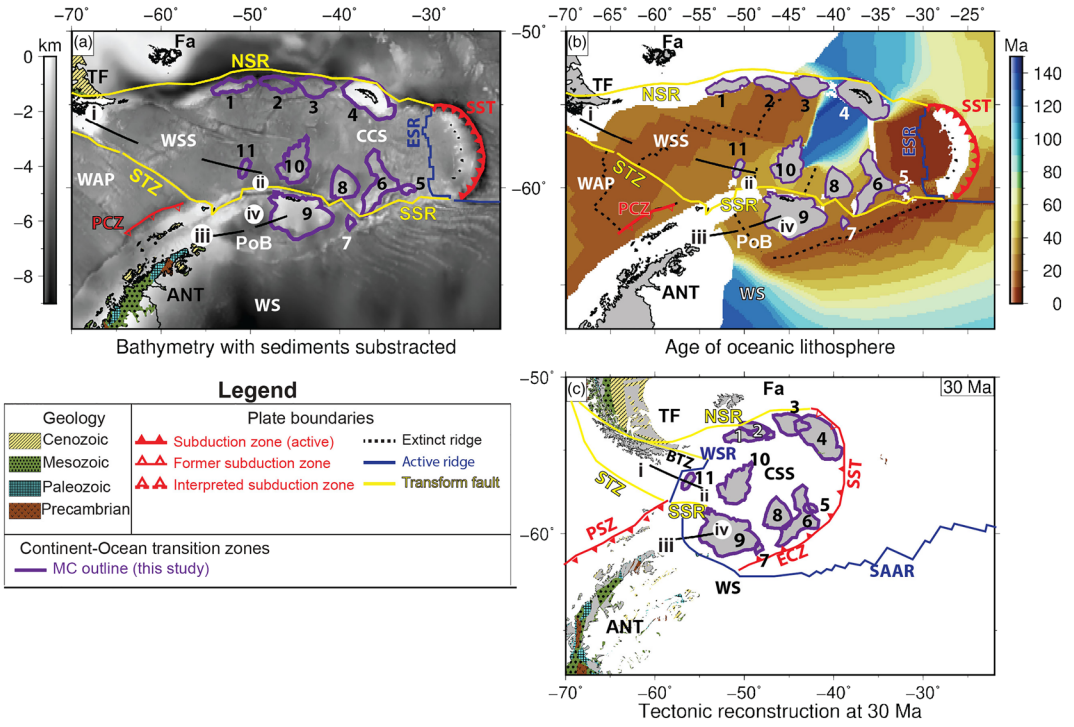

Figure 5. Geological models and bathymetric observations for the Scotia Sea. (a) Bathymetry with sediments subtracted (no backstripping) and onshore geology. (b) Oceanic age grid of the various basins in the Scotia Sea. (c) Tentative tectonic reconstruction of the pre-breakup configuration of the Scotia Sea. Microcontinents: 1 = Davis Bank; 2 = Barker Bank; 3 = Shag Rocks; 4 = South Georgia Microcontinent; 5 = Herdman Bank; 6 = Discovery Bank; 7 = Jane Bank; 8 = Bruce Bank; 9 = South Orkney Microcontinent; 10 = Pirie Bank; 11 = Terror Rise; Other abbreviations: ANT = Antarctica; WS = Weddel Sea; ESR = East Scoti a Ridge; NSR = North Scotia Ridge; SSR = South Scotia Ridge; TF = Tierra del Fiego; Fa = Falkand Islands; STZ = Shackelton Fractue Zone; WAP = West Antarctic Plate; PSZ = Pacific Subduction Zone; BTZ = Burdwood Transform Fault; WSR = West Scotia Ridge; CCS = Central Scotia Sea; ECZ = Endurance Subduction Zone; SST = South Sandwich Trench.

Some authors suggest that northwest to north directed subduction continued, but extension relocated and resulted in back-arc opening to the south China Sea (Sibuet et al., 2016; Wu et al., 2016). Other authors proposed that the Proto South China Sea subducted southward beneath NE Borneo and Palawan and the South China Sea basin opened NW of it (Figure 3c) (Bai et al., 2015; Zahirovic et al., 2014). No conclusive evidence for either model exists, but observations and dating on Borneo point to a southward directed Paleogene subduction (Hall & Breitfeld, 2017). However, more data are needed to better understand these scenarios.

The South China Sea experienced three phases of rifting since the late Cretaceous, two of which occurred during the Cenozoic (Cullen et al., 2010). Rifting from Paleocene to Eocene was widespread, as documented by the structure of the South China Sea margins (Cullen et al., 2010; Franke et al., 2014). Subsequent rifting from the late Eocene to early Miocene was more localized, and resulted in continental breakup and initiation of seafloor spreading in the South China Sea basin (Cullen et al., 2010; Franke et al., 2014; Li et al., 2014; Sibuet et al., 2016).

The present-day South China Sea has two main subbasins: the east and southwest subbasins (Figure 3) (Li et al., 2014). Recent IODP drilling, detailed analysis of deep tow magnetic data, and interpretation of seismic reflection data indicate that breakup in the (northern) east subbasin occurred in early Oligocene times (Franke et al., 2014; Li et al., 2014). Extension propagated westward, as evidenced by continental rifting in the Xisha trough (Figure 3a) (Sibuet et al., 2016). In late Oligocene–early Miocene times, a southward ridge jump occurred in the east subbasin which terminated the extension in the Xisha trough and spreading along the northern margin (Figure 3b) (Li et al., 2014; Sibuet et al., 2016) and initiated seafloor spreading in the southwestern subbasin (Li et al., 2014; Sibuet et al., 2016). This mid-ocean ridge further propagated in a south-westerly direction, creating the distinctive V-shape of the South China Sea southwest subbasin

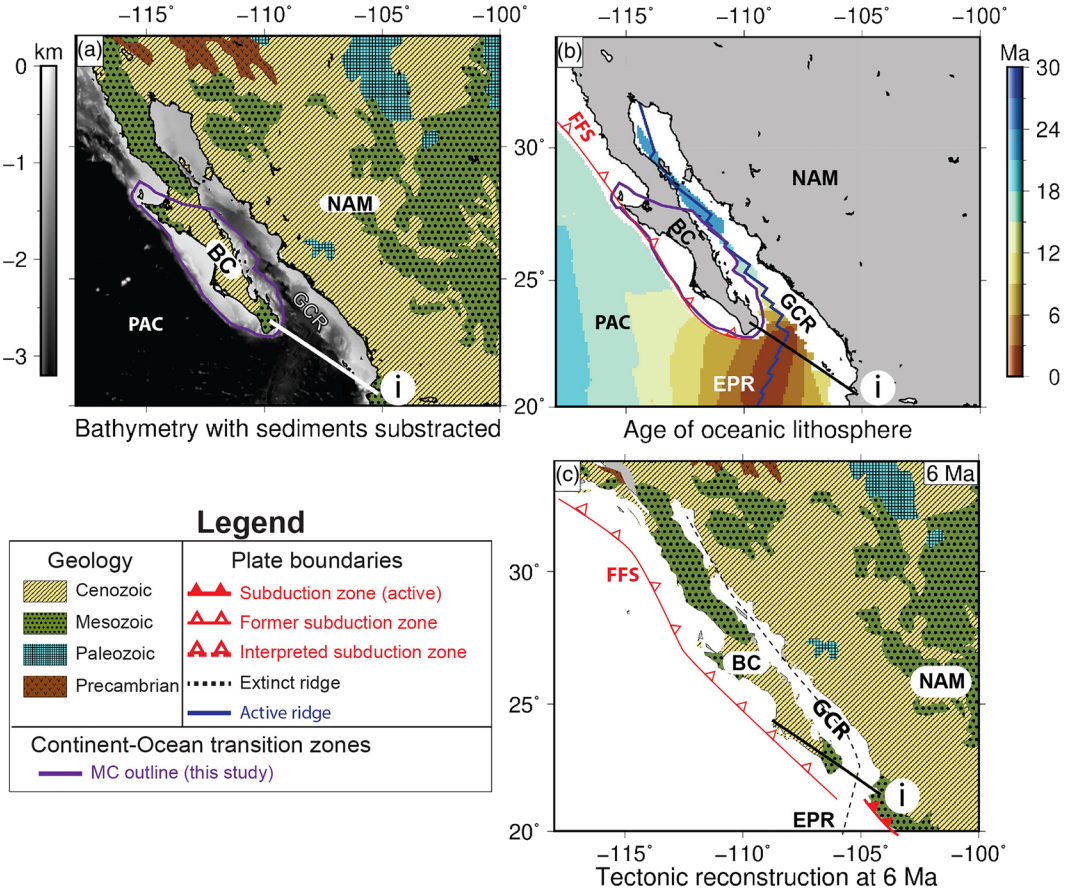

Figure 6. Geological models and bathymetric observations for Gulf of California region. (a) Bathymetry with sediments subtracted (no backstripping) and onshore geology. (b) Oceanic age grid of the various basins in the Gulf of California region. (c) Tentative tectonic reconstruction of the pre-breakup configuration of the Gulf of California. NAM = North American plate; BC = Baja California; GCR = Gulf of California Ridge; EPR = East Pacific Rise; FFS = Farallon Subduction zone; PAC = Pacific plate.

(Franke et al., 2014; Sibuet et al., 2016). Opening of the South China Sea detached the Reed Bank, Dangerous grounds, and a continental block comprised of NE Palawan and SW Mindoro from the South Chinese Margin (Figure 3). During its lifetime, extension and spreading directions in the South China Sea rotated from N175°, via N165° to N145° (Sibuet et al., 2016). Spreading in the South China Sea ceased in the middle Miocene (Figure 3b) and this event is often correlated with the choking of the Proto South China Sea subduction zone by a block with thick crust (e.g., NE Palawan and SW Mindoro) (Hall & Breitfeld, 2017; Sibuet et al., 2016; Yumul et al., 2003).

2.3. The Central Mediterranean Sea

The Mediterranean Sea region has experienced a long and complex tectonic evolution since the Paleozoic. The opening and closing of various oceanic basins resulted in an amalgamation of terranes with different ages and compositions (Figure 4) (Dewey & Sengör, 1979; Vissers et al., 2013; von Raumer et al., 2003).

The Africa-Eurasia/Iberia convergence played the main role in the Cenozoic evolution of this region. Convergence of Iberia with Eurasia resulted in the formation of the Pyrenean orogeny which, at the time, extended eastward into southern France as evidenced by basement thrusting (Lacombe & Jolivet, 2005). Further east, convergence between the Adriatic microplate and Eurasia created the Alps (Schmid et al., 2017; Turco et al., 2012).

Around Oligocene times, the northward subducting African slab segmented into the Calabrian and Balearic slabs which started to rollback independently (Figure 4c) (Faccenna et al., 2001; Seton et al., 2012;

van Hinsbergen et al., 2014). During this period of slab rollback the continental Corsica-Sardinia block was detached from Eurasia and the Liguro-Proven_x004AB;al back-arc basin was formed (Advokaat et al., 2014; Gattacceca et al., 2007; Seranne et al., 1999). Just before continental breakup between Eurasia and the Corsica-Sardinia block, the Adriatic microplate was colliding with the southern Eurasian margin, resulting in simultaneous subduction of oceanic and continental material (Figure 4) (Turco et al., 2012; van Hinsbergen et al., 2014). This may have triggered or contributed to continental breakup of the southern Eurasian margin and subsequent seafloor spreading in the Liguro-Proven_x004AB;al basin in early Miocene time (Figure 4b) (Faccenna et al., 1997). As a consequence, the Corsica-Sardinia block rotated counterclockwise ca. 45–50° around an Euler pole located just north of Corsica (Figure 4) (Advokaat et al., 2014; Gattacceca et al., 2007). Seafloor spreading in the Liguro-Provençal basin was active from early (21 Ma) to middle Miocene (Faccenna et al., 1997). After a 6 Myr quiet period, at 10 Ma the extension relocated east of the Corsica-Sardinia microcontinent, initiating the formation of the Tyrrhenian basin (Faccenna et al., 2001). This relocation of extension terminated the relative motion of the Corsica-Sardinia microcontinent with respect to Eurasia, leaving it isolated in the Central Mediterranean in its present-day position.

2.4. The Scotia Sea

The Scotia Sea region is situated between the Antarctic Peninsula and the southern tip of South America. Its Cenozoic evolution has been controlled by the interaction between the Antarctic and South American plates. Although the tectonic evolution of the region is still debated, several scenarios have been proposed (Dalziel et al., 2013; Eagles & Jokat, 2014).

The pre-breakup setting of the region is controversial (Brown et al., 2006; Eagles & Jokat, 2014; Müller et al., 2008). Dalziel et al. (2013) suggest that the South Georgia microcontinent was located south of Tierra del Fuego from Jurassic to Cenozoic times. In contrast, Eagles (2010a) proposed that it was located in a more internal part of Gondwana and that the formation of the Central Scotia Sea oceanic crust was associated with Gondwana breakup. According to Eagles (2010), the South Georgia microcontinent was located adjacent to the Falkland Islands in early Eocene times (Figure 5). At that time interval, the continental fragments that are presently distributed along the South Scotia Ridge (Figure 5) were clustered north of the South Orkney microcontinent, and are considered to have been part of the East Antarctic Plate (Eagles & Jokat, 2014). East of this assemblage, the Endurance subduction zone was active since the early Paleocene (Barker et al., 1991; Eagles, 2010b), subducting oceanic lithosphere from the northwest Weddell sea beneath the South Orkney microcontinent (Figure 5c).

During middle Eocene times, a rotation of the South American-Antarctica plate system drove southeast-directed trench retreat of the Endurance trench and/or changes along the Burwood transform zone. This resulted in the initiation of rifting in the Powel Basin (King & Barker, 1988), between the Antarctic Peninsula and the South Orkney microcontinent, and spreading between the Pirie and Bruce Banks (Figure 5) (Barker et al., 2013; Eagles et al., 2006).

At the start of Oligocene times, the extension relocated westward between the Pirie Bank and the Terror Rise (Figure 5) (Eagles & Jokat, 2014). In the middle Oligocene extension once again relocated westward to the West Scotia Ridge, between Tierra del Fuego and the Terror Rise (Figure 5) (Eagles et al., 2006). Also in the middle Oligocene, breakup occurred in the Powell basin and the Endurance subduction zone lengthened northward toward South Georgia (Figure 5c) (Barker, 1995; Eagles & Jokat, 2014). This led to the abandonment of the Burwood transfer zone in favor of the North Scotia Ridge and the formation of microcontinents by the transfer of the various northern continental fragments from the South American plate to the Scotia plate (Eagles & Jokat, 2014).

Collision of ridge segments from the South American-Antarctic ridge system with the Endurance subduction zone resulted in the cessation of spreading along the Powell ridge around early Miocene (Figure 5b) (Barker, 1995; Eagles & Livermore, 2002). This resulted in the formation of the South Scotia Ridge, which acted as a plate boundary between the Scotia Sea and Antarctic plates. After this reorganization, the South Orkney microcontinent and the Bruce bank started to diverge from the Jane and Discovery banks as the Proto-East Scotia Ridge and associated Sandwich plate were established in a back-arc setting (Figure 5b) (Vanneste & Larter, 2002). Collision of the South American-Antarctic Ridge with the South

Sandwich trench ended the extension along the southern part of the Proto-East Scotia Ridge (Eagles & Jokat, 2014). The newly formed Sandwich plate quickly accommodated the eastward directed trench roll-back of the South Sandwich trench. Spreading along the East Scotia Ridge resulted in a cessation of extension along the West Scotia Ridge in the late Miocene (Figure 5b) (Eagles et al., 2005). Back-arc spreading along the East Scotia Ridge is still active today, accommodating the eastward trench retreat of the South Sandwich Trench (Smalley et al., 2007).

2.5. The Gulf of California

The western margin of the North American plate was a long-lived convergent margin since the Jurassic and experienced an amalgamation of numerous terranes (e.g., Wright et al., 2016). When the active mid-ocean ridge between the Pacific and Farallon plates reached this convergent margin, a transtensional motion followed by ridge propagation into the continental margin led to the gradual detachment of Baja California from North American plate (Atwater, 1970; Atwater & Severinghaus, 1989).

The exact evolution of Gulf of California system (Figure 6) from a convergent to an extensional system has been the subject of numerous studies. The classical view is that continental rifting in the Gulf of California initiated in the middle Miocene and quickly transitioned to seafloor spreading during the late Miocene–early Pliocene (Lizarralde et al., 2007; Umhoefer, 2011). It is thought that this quick transition from continental rifting to breakup was due to the combination of an already existing hot and weak crust between the two strong crustal blocks of the Baja California and the Mexican mainland, and relatively rapid and very oblique plate motions between the North American and Pacific plates (Umhoefer, 2011).

Recently, Ferrari et al. (2018) suggested an alternative scenario postulating that extension in the region initiated in the middle Eocene via a wide continental rift adjacent to the southern Basin and Range province. The initiation of rifting was tentatively connected to the decrease in the North-American-Farallon convergence rates and the presence of slab windows in the mantle (Ferrari et al., 2018). This plate velocity decrease led to changes in plate boundary forces and the availability of fertile mantle beneath the Gulf of California. From the early to middle Miocene, extension localized in a narrow rift at the approximate location of the present-day Gulf of California (Ferrari et al., 2018). In middle Miocene time, cessation of subduction west of Baja California led to a change in the stress state that resulted in transtension/extension of the Gulf of California.

The available tectonic models agree that continental breakup occurred in the southern Gulf of California during the Pliocene (Lizarralde et al., 2007; Umhoefer, 2011). The transtensional rifting was diachronous and varied along strike from narrow to wide rifts (Lizarralde et al., 2007). Although the Baja Californian microcontinent has yet to detach from the North-American mainland, the continued activity in the Gulf of California suggests that separation might occur in the future. As such, Baja California can be considered a “proto-microcontinent.”

3. Present-Day Microcontinent Structure From Geophysical Data and Geological Models

Each region described in the previous section hosts one or more microcontinents that formed in association with a subduction system. In order to understand the formation of these microcontinents we need a comprehensive overview of their present-day structure, especially their rifted margins and the parent-continent conjugate margins. In the following, we will present a characterization of the rifted margins of selected microcontinents based on publicly available geophysical and geological data and models.

We use free-air gravity anomalies from Sandwell et al. (2014) and Bouguer gravity anomalies from the World Gravity Map (Balmino et al., 2012; Bonvalot et al., 2012) to investigate the margin architectures. Both data sets have a 1° spatial resolution. For inspecting magnetic anomalies, we use the gridded magnetic data from the NGDC marine trackline database (http://geomag.org/models/wdmam.html). These data are line-leveled and projected to sea-level according to the procedure described by Paterson and Reeves (1985). Where possible, published models of crustal thickness are also considered. In the Mediterranean we utilize EPcrust model (Molinari & Morelli, 2011), and in the Gulf of California CRUST1.0 is used (Laske et al., 2012). For all other regions, (global) crustal thickness models have an inadequate resolution. Instead, we use various local seismic studies to constrain crustal thickness where possible.

We also inspect few tomographic models for visually identifying the subducted slabs that may have been connected to subduction processes that led to microcontinent formation. Slab sinking velocities in the upper mantle are generally considered to be slightly less or equal to the Stokes sinking velocity of a sinking slab, which are around 2–7 cm/year (Capitanio et al., 2007). A simple calculation suggests that a slab sinking at 5 cm/year will arrive at the 660 km discontinuity about 13 Myr after the slab starts sinking. Due to the increased viscosity in the lower mantle, sinking velocities of slabs in the lower mantle are significantly slower at roughly 1.2 cm/year (Goes et al., 2008). Note that slabs may also deform and stall at the transition zone between upper and lower mantle, and a slab thickening by a factor of 2–3 in the viscous lower mantle is also expected (Gaherty & Hager, 1994).

Since all microcontinents discussed in this study formed in the Cenozoic time, and most of them in the last 30 Ma (see section 2), we expect to see the slabs in the upper mantle and upper lower mantle. For a qualitative inspection of the subducted slabs, and without the intention to assign exact ages to identified slabs, we have chosen the UU-P07 seismic tomographic model by Amaru (2007). The UU-P07 model has a good resolution in the upper mantle (0.4° laterally). The model was obtained by the use of 3-D reference models which are based on travel time residuals and independent models based on surface waves, normal models, and long period body waves. Other tomographic (DETOX-P3, Hosseini et al., 2019; MITP08, Li et al., 2008; and TX2019slab, Lu et al., 2019) are shown for comparison in the supporting information (Figures S2–S6).

We inspect the microcontinent margins and their conjugates and attempt to characterize the transition from continental to oceanic domain (continent-ocean boundary or transitional domain, COB or COT) expressed in geophysical data along selected profiles perpendicular on these margins. We consider the inboard COT location, where transitional crust starts to replace extensional continental crust, as the outer boundary of the relevant microcontinent. Where available, we show previously published COB/COTs, and adopt their outboard (where oceanic crust starts) COTs or COB interpretation if no inboard COT is available. Although identification of COBs based on potential field data may be less precise (Eagles et al., 2015), it does allow us to make a rough first order estimation of the microcontinent size and constrain a first order margin architecture. By tentatively identifying the first magnetic anomaly associated with sea-floor spreading, we obtain a first order estimate of the outboard limit of interpreted transitional crust. The conjugated profiles and identified COB/COTs are subsequently reconstructed to pre-breakup positions, allowing us to identify the symmetry (or lack of) of the margin morphology. Finally, we gather information and make a rough estimation of the continental crust volumes detached from active margins due to subduction processes.

3.1. Microcontinents in the Coral Sea

Located off the northeastern margin of Australia (Figures 1 and 2), the Louisiade Plateau is one of several pieces of continental lithosphere originally attached to this margin (see section 2.1). It is roughly 270 × 470 km in size and is separated from the Australian margin by the Coral Sea oceanic crust (Figure 2). While the Louisiade Plateau is submerged, the crustal nature of this microcontinent is inferred from geophysical data. Seismic reflection data show a similar structure as the conjugate continental Queensland plateau situated on NE Australian margin (Ewing et al., 1970; Feary et al., 1993; Taylor & Falvey, 1977). Dredged rocks from various plateaus in the NE Coral Sea basin support this continental nature (Hoffmann & Exon, 2008) and tectonic reconstructions indicate their origin from NE Australia (Figure 2c) (Gaina et al., 1999).

Continent-Ocean boundaries for the Coral Sea have been published and are included on the maps in Figures 2 and 6. The COBs of the Coral Sea and neighboring Rennell and Louisiade troughs are mainly interpreted based on gravity and magnetic anomaly data, and we have adopted the microcontinents outline from Seton et al. (2016) which is partially based on Gaina et al. (1999). This interpretation seems to hold against global geophysical data shown in our maps (Figure 7).

The Louisiade Plateau margin shows a smooth geometry (Figure 7e, profile ii). Both the Queensland plateau (Figure 7e, profile i) and the Louisiade plateau (Figure 7e, profile ii) margins have a subtle shelf break around the COB. The Queensland Plateau has a slightly steeper gradient in the “no-sediment bathymetry” and gravity data when compared to the conjugate Louisiade Plateau. This could indicate a slight asymmetry in the conjugate margins for these two selected locations. There appears to be a roughly 50 km wide gap between the interpreted COB of the Louisiade plateau and the first interpreted seafloor magnetic anomaly

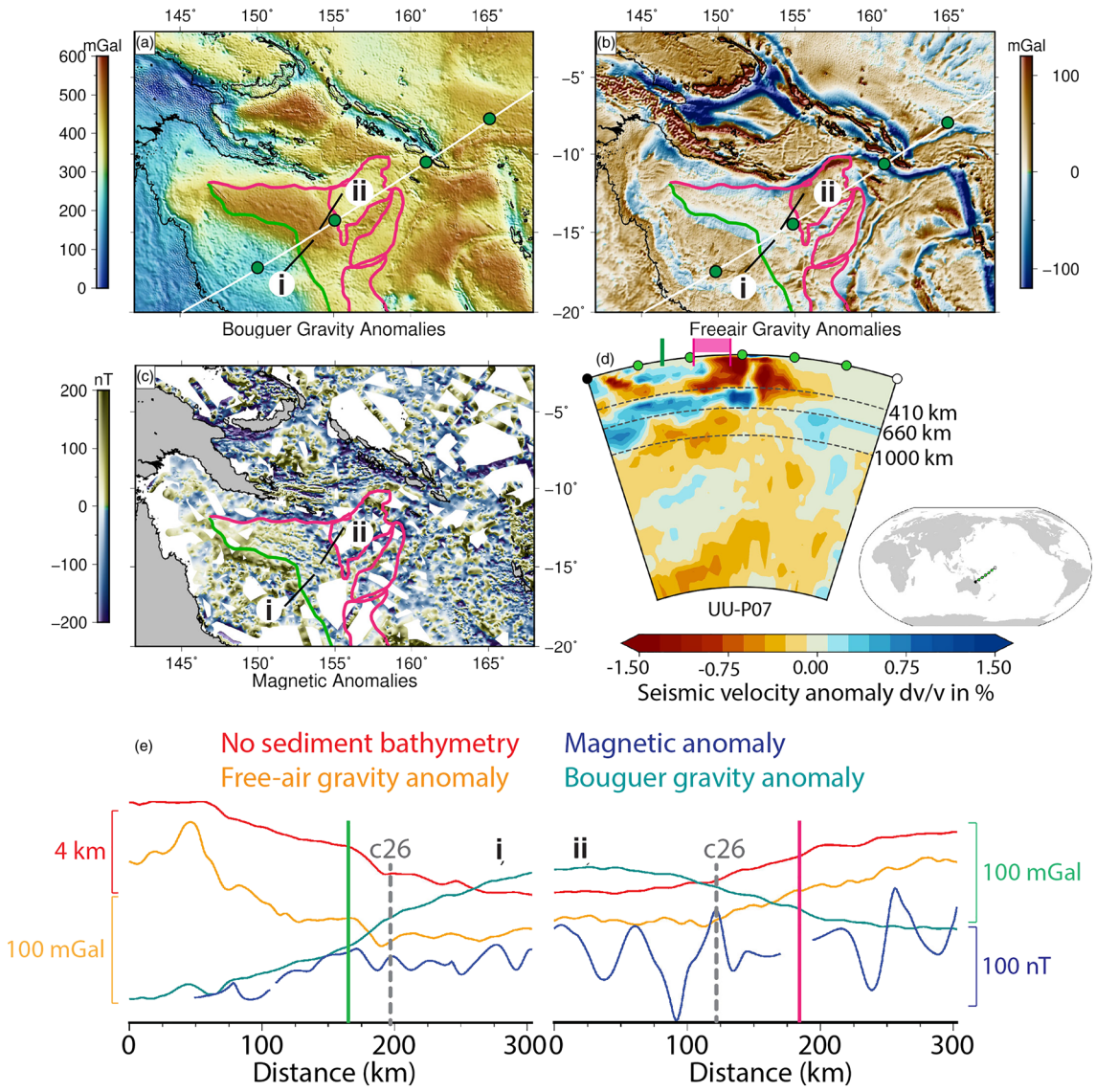

Figure 7. Geophysical data and models for the Coral Sea region. Legend as in Figure 2. Note the COB of the Coral Sea basin and the various microcontinents. The white line in panels (a) and (b) represents the profile along which the tomographic section is extracted. (a) Bouguer Gravity Anomalies. (b) Free-air Gravity Anomalies. (c) Magnetic anomalies, first spreading anomalies based on Gaina et al. (1999). (d) Seismic tomography section from UU-P07 crossing the Coral Sea region. (e) Profiles of geophysical data extracted along profiles i and ii. See Figures 2 and 7a–7c for location (black thin lines).

in this region (C26), and a distance of about 30 km between the COB and identified seafloor magnetic anomalies on the conjugate Queensland plateau (Figure 7e). Taking into account the uncertainties in identified COBs, we consider that the seafloor spreading at this specific location may have started slightly before C26. Following continental breakup, the formation of conjugate oceanic flanks was relatively symmetric.

Vintage seismic refraction data as well as gravity data and modeling suggest that the crustal thickness of the Louisiade plateau is around 20 km (Ewing et al., 1970). The conjugate Queensland plateau has a crustal thickness of around 25–28 km and the oceanic crust flooring the Coral Sea is around 7 km thick (Taylor & Falvey, 1977). Crustal thickness data for the Mellish Rise and the Kenn Plateau are poorly constrained. The regional crustal model from Segev et al. (2012) and Crust1.0 (Laske et al., 2012) indicate these plateaus have crustal thickness of around 7–11 km. The values for the Bouguer gravity anomalies on the various submerged plateaus are only slightly lower than the anomalies in the oceanic Coral Sea Basin (Figure 7a). This could indicate that the continental crust there is relatively thin.

Table 1
(a) Table Detailing the Data Used in Calculations of Total Continental Crustal Area and Volume; (b) Global Continental Crustal Area and Volume and Total Continental Crustal Area and Volume for Each Region Described in This Paper; (c) The Amounts of Continental Crust in Classic and Subduction Associated Microcontinents, Normalized to Global non-Cratonic Continental Crust Area and Volume

(a) Crustal area and volume for each MC-CF

Region	MC-CF	Area (km^2)	Thickness (km)	Source	Volume (km^3)
California	Baja California Microplate	1.70E + 05	18	6	3.10E + 06
Coral Sea	Louisiade Plateau	1.29E + 05	20	1	2.57E + 06
	Mellish Rise	8.10E + 04	10	2	8.10E + 05
	West Torres Plateau	4.40E + 04	11	2	4.84E + 05
	Kenn Plateau	7.33E + 04	11	2	8.07E + 05
South China	Macclessfield bank	9.39E + 03	16	1	1.50E + 05
	Reed Bank	2.00E + 04	24	1	4.79E + 05
Scotia	Barker Bank	1.90E + 04	18	4	3.42E + 05
	Bruce Bank	2.45E + 04	18	4	4.40E + 05
	Davis Bank	2.12E + 04	17	4	3.60E + 05
	Discovery Bank	2.07E + 03	25	5	5.17E + 04
	Herdman Bank	3.37E + 03	18	4	6.06E + 04
	Jane Bank	2.07E + 03	18	4	3.72E + 04
	Pirie Bank	3.75E + 04	18	1	6.75E + 05
	South Georgia Microcontinent	6.63E + 04	19	4	1.26E + 06
	South Orkney Microcontinet	7.31E + 04	24	1	1.75E + 06
	Shag Rocks	2.78E + 04	18	4	5.00E + 05
	Terror Rise	5.14E + 03	17	4	8.74E + 04
Mediterranean	Corsic-Sardinia	1.11E + 05	22	3	2.42E + 06

b) Cont. Crust area and volume—Global

	Area (km^2)	**Volume (km^3)**
Total continental crust	1.93E + 08	6.96E + 09
Cratonic crust	2.80E + 07	1.10E + 09
Non-cratonic continental crust	1.65E + 08	5.86E + 09
Classic microcontinents	3.22E + 06	5.08E + 07

Crustal area and volume for each region

Region	**Area (km^2)**	**Volume (km^3)**
California	1.70E + 05	3.10E + 06
Coral Sea	3.27E + 05	4.67E + 06
South China Sea	2.93E + 04	6.29E + 05
Scotia Sea	2.82E + 05	5.57E + 06
Mediterranean	1.11E + 05	2.42E + 06

Crustal area and volume per MC type

Type	**Area (km^2)**	**Volume (km^3)**
Microcontinent	6.09E + 05	1.02E + 07
Cont. fragment	1.40E + 05	3.05E + 06
Proto MC-CF	1.70E + 05	3.10E + 06
Total	**9.19E + 05**	**1.64E + 07**

c) Percentage of non-cratonic continental crust

Feature	**Area (%)**	**Volume (%)**
Classic microcontinents	1.95	0.87
Subduction microcontinents	0.56	0.28
All microcontinents	**2.51**	**1.15**

Note. (a) See the text for details regarding the calculation. Sources for crustal thickness assumptions are provided. Data sources: 1 = Seismic refraction data; 2 = Crust1.0 (Laske et al., 2012); 3 = EPcrust (Molinari & Morelli, 2011); 4 = S wave velocity model; 5 = Surface wave tomography; 6 = Seismic receiver functions.

Utilizing the published COBs and microcontinent outlines, we find that the total area of the microcontinent-like submerged plateaus offshore NE of Australia (Louisiade, Kenn and West Torrest Plateaus, and the Mellish Rise) is ~3.27×10^5 km^2. Using a thickness of 20 km for the Louisiade Plateau and 11 km for the other microcontinents, we find a total crustal volume of microcontinents in the Coral Sea region of ~4.75×10^6 km^3. A detailed overview of the areas, thicknesses, and volumes of each microcontinent can be found in Table 1.

A vertical profile extracted from the selected seismic tomography model shows a fast anomaly below Australia and the Coral Sea situated between 410 and 660 km (Figures 7d and S2). The slab appears to be

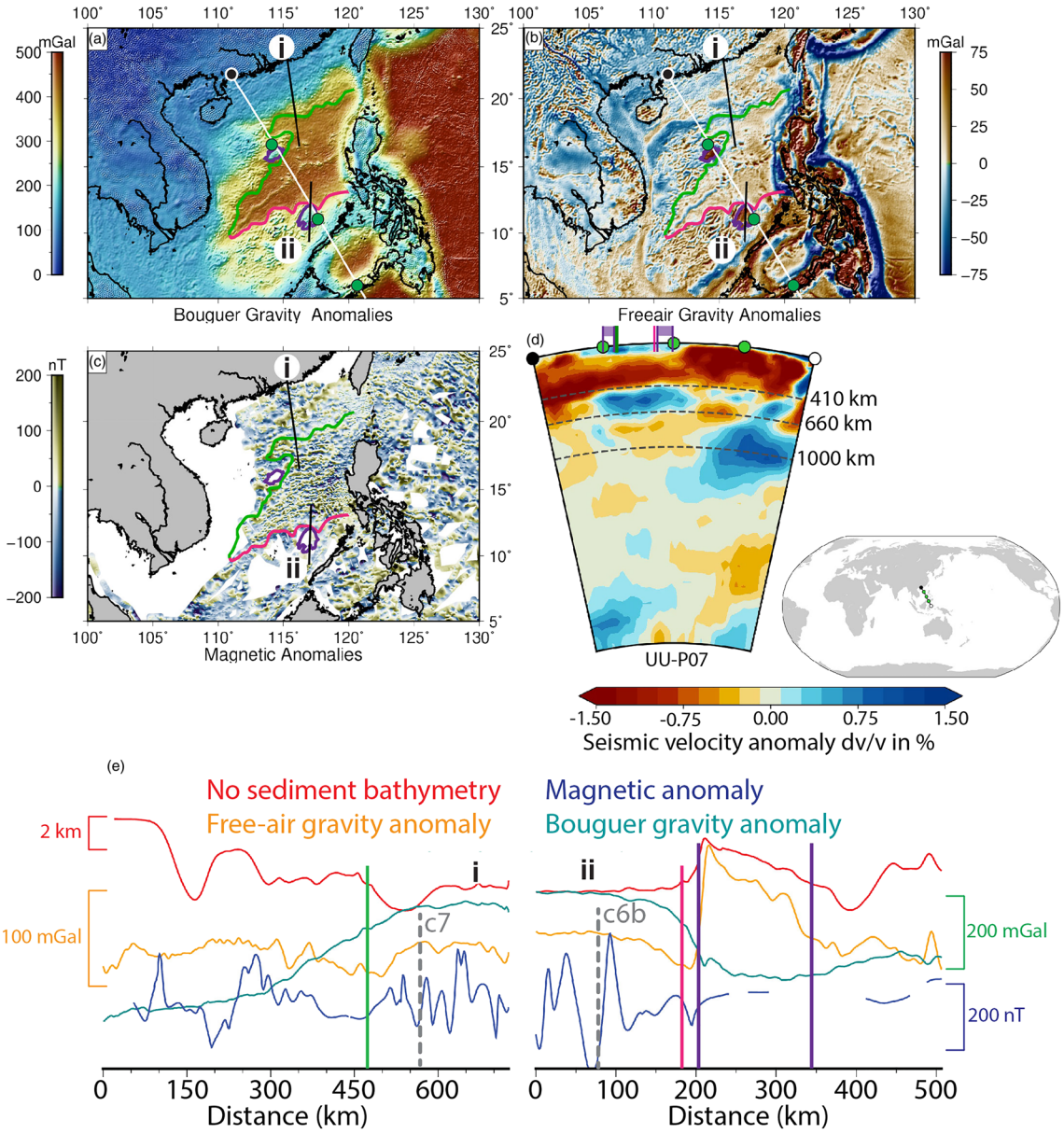

Figure 8. Geophysical data and models for the South China Sea region. Legend as in Figure 3. Note the COB of the South China Sea basin and the various microcontinents. The white line in panels (a) and (b) represents the profile along which the tomographic section is extracted. (a) Bouguer Gravity Anomalies. (b) Free-air Gravity Anomalies. (c) Magnetic anomalies, first spreading anomalies based on Barckhausen and Roeser (2004). (d) Seismic tomography section from UU-P07 crossing the South China Sea region. (e) Profiles of geophysical data extracted along profiles i and ii. See Figures 3 and 8a–8c for location (black thin lines).

detached from the surface and partially draped on the 660 km discontinuity toward the Australian continent. It underlies the Coral Sea basin, indicating a southwestward subduction that may have caused the formation of this basin. Below NE Australia the slab appears to penetrate into the lower mantle which may point to an older age of the slab, early Cenozoic or late Cretaceous. However, if the Coral Sea formed due to a NE oriented subduction (i.e., Whattam et al., 2008), another steeper, detached slab is visible in the upper lower mantle under the Pacific plate. Another slab dipping southward under the Australian continent could be identified in the lower mantle below 1,000 km, indicating episodic subduction under this continent at least since the Cretaceous time (Figure 7d).

3.2. Microcontinents in the South China Sea

During the opening of the South China Sea basin, the submerged Reed bank in the NE Palawan and SW Mindoro continental blocks detached from the Chinese mainland (Figure 3) (Bai et al., 2015; Sibuet et al., 2016; Taylor & Hayes, 1980). The submerged Macclesfield bank is still attached to the Chinese continental margin via extended continental crust (Figures 3 and 8). The Reed and Macclesfield banks have an approximate size of 160 × 80 and 200 × 130 km, respectively. Evidence for their continental nature is provided by various seismic refraction experiments (Hutchison, 2004; Pichot et al., 2014) as well as ODP drilling (Shipboard Scientific Party, 2000) and dredging (Kudrass et al., 1986).

Due to its high hydrocarbon potential, the South China Sea has been extensively surveyed. Consequently, several COB interpretations exist and the margin architecture is relatively well known. We utilize the South China Sea COB identification from Pichot et al. (2014), which is shown on the maps in Figure 3. This interpretation is primarily based on seismic reflection and refraction data (Franke et al., 2014; Pichot et al., 2014). Our COB interpretation based on available geophysical data agrees with published COBs based on seismic data (Figure 8). While a full set of COT boundaries for the entire South China Sea has not been published yet, there is a general consensus in the literature that a COT is relatively narrow (~30 km) in comparison with the width of the rifted margins themselves (400–800 km).

Due to the fact that South China Sea sits on a lower plate that subducts southeastward, the exact extent of its southern margin is unclear. However, the northern continental rifted margin is preserved and shows lateral variation in width (Figures 3a and 8). The eastern part of the northern rifted margin has a width of around 400 km, while south of Hainan the rifted margin is almost 800 km wide (Pichot et al., 2014) (Figures 3a and 8). Free-air gravity anomalies show a relatively smooth trend for the northern margin of the eastern subbasin, while the South China Sea's southern margin and the northern margin of the SW subbasin show a shorter wavelength variation, which may be correlated to brittle surface faults (Franke et al., 2014) (Figure 8b).

Geophysical data extracted along the profiles crossing the Chinese continental margin and the Reed bank show clear shelf breaks toward the oceanic South China Sea basin (Figure 8e). Toward the southern end of the Reed bank, the gradients in the geophysical data are less steep and the sharp northern boundary is not seen in the south. This suggests that the sharp transition from continental to oceanic crust is related to the process that localized extension during continental breakup.

Although the COT is interpreted to be abrupt, the magnetic data extracted along the profiles shows a ca. 100 km wide zone between the interpreted COB and first magnetic anomaly (C6b) (Figure 8e). Other authors observed a similar wide COT in NW Palawan, where it was interpreted to be related to magma starved extension resulting in mantle exhumation (Franke et al., 2011). The northern South China Sea margin also has a transitional region of 75 km wide (Figure 8e). The formation of these transitional zones may be related to a slow-down in extension after breakup or a period of mantle exhumation that may have preceded the formation of normal oceanic crust in the South China Sea.

Crustal thickness of continental blocks in South China Sea is constrained by wide-angle seismic refraction data and suggests values of around 24 km for the Reed Bank (Ruan et al., 2011) and 16 km for the Macclesfield bank (Huang et al., 2019). The conjugate northern margin has a crustal thickness of around 20–24 km, inferred from seismic refraction data (Pichot et al., 2014; Wang et al., 2006; Wu et al., 2012). Using the published COB from Pichot et al. (2014), we find that the total crustal area of the Reed and Macclesfield Banks is ~2.93×10^4 km^2. A crustal thickness of 24 and 16 km for the Reed and Macclesfield banks, respectively, yields a total crustal volume ~6.29×10^5 km^3 for the microcontinents found in the South China Sea region. A detailed overview of the areas, thicknesses, and volumes of South China Sea microcontinents can be found in Table 1.

Seismic tomography along a vertical profile crossing the South China Sea shows a fast anomaly between 410 and 660 km, and another wider anomaly to the south in the upper lower mantle below the Celebes Sea basin (Figures 8d and S3). Both anomalies could be linked to the two stages opening of the South China Sea (see section 2). The fast anomaly in the shallow lower mantle could be the detached proto-South China Sea slab, but the complex history of this region cannot rule out a different interpretation (Figure 8d).

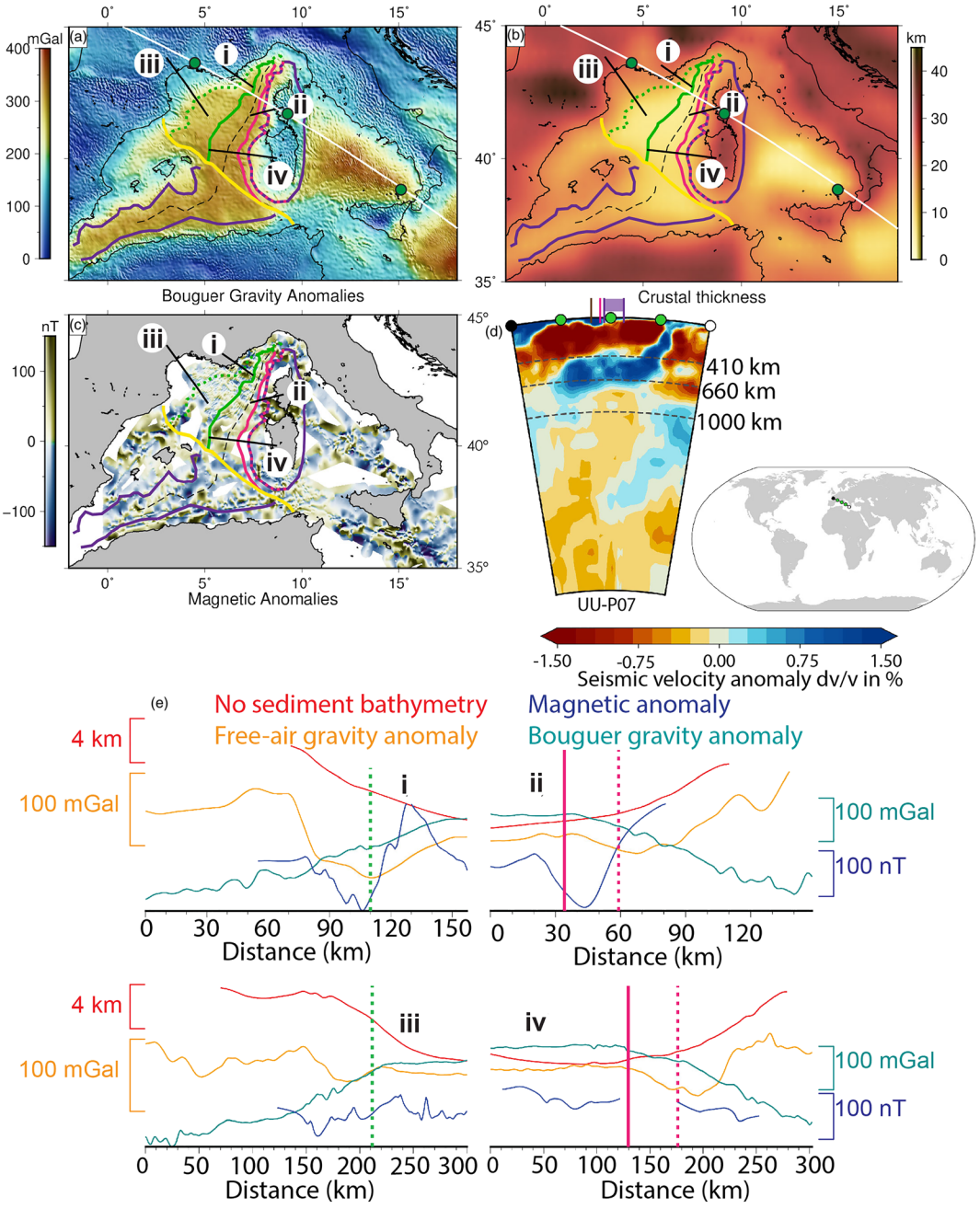

Figure 9. Geophysical data and models for the Central Mediterranean region. Note the COB of the Liguro-Provençal basin and the Corsica-Sardinia block. Legend as in Figure 4. The white line in panels (a) and (b) represents the profile along which the tomographic section is extracted. (a) Bouguer Gravity Anomalies. (b) Crustal thickness from EPCrust. (c) Magnetic anomalies. (d) Seismic tomography section from UU-P07 crossing the Central Mediterranean region. (e) Profiles of geophysical data extracted along profiles i, ii, iii, and iv. See Figures 4 and 9a–9c for location (black thin lines).

3.3. Microcontinents in the Central Mediterranean Sea

An excellent bathymetric fit of the margins (Bache et al., 2010), paleomagnetic constraints (Advokaat et al., 2014; Gattacceca et al., 2007), and onshore Hercynian and Alpine geology (di Rosa et al., 2017; Faccenna et al., 2004; Gueydan et al., 2017; Rossi et al., 2009) prove the continental origin of the Corsica-Sardinia block which detached from the southern margin of France after opening of the Liguro-Provençal basin (see also section 2.3). This continental block is roughly 230 × 470 km in size, is flanked

by the Liguro-Provençal basin to the west and the Tyrrhenian basin to the east, and toward the north is attached to the Adriatic microplate via extended, submerged, continental crust (Figure 9).

Based on seismic reflection data, in combination with gravity and magnetic observations, Rollet et al. (2002) published a map delineating the complete continent-ocean transition zone (COT) with both inboard and outboard COT boundaries for the Ligurian basin (Figures 4 and 9). These where subsequently expanded upon by Jolivet et al. (2015) who used a new seismic reflection profile. As these COT interpretations are well constrained and in agreement with our selected geophysical data, we utilize them in Figures 4 and 9. As the available COT interpretation does not cover the entire Corsica-Sardinia block, we have extended this interpretation of inboard COT by using the geophysical data described previously in the manuscript (Figures 4a and 9). The high amplitude magnetic anomalies are likely related to volcanic intrusions, as also suggested by Rollet et al. (2002) (Figure 9c).

The margins of the Corsica-Sardinia and their Eurasian conjugates have been extensively studied using seismic reflection and wide-angle refraction data (Gailler et al., 2009; Jolivet et al., 2015; Rollet et al., 2002). Both the Eurasian and Corsica-Sardinia margins show a progression of crustal types from a thinned continental margin to transitional crust which changes into a typical oceanic material in the center of the basin (Gailler et al., 2009). Geometrically, however, the Liguro-Provençal basin as well as its margins are asymmetric (Figures 4a and 9).

General asymmetry of the Liguro-Provençal basin is visible in the eastward lateral offset of the high Bouguer gravity anomalies (Figure 9a). The margin in the Gulf of Lyon is around 150 km wide, while the Sardinian margin is around 100 km wide (Bache et al., 2010; Gailler et al., 2009). The Corsican margin is roughly 70 km wide and the Ligurian margin has a width of circa 40 km. The Ligurian COT is around 40 km while the Corsican COT is around 50 km (Contrucci et al., 2001; Rollet et al., 2002). Note that the available age grid for the Central Mediterranean is not accurate (Figure 4). We suggest that our new interpretation of COT and tentative location of an extinct mid-ocean ridge can be used in the future to amend the existent age grid.

Crustal thickness from EP crust is around 5 km or less in both the Liguro-Provençal and Tyrrhenian basins. The Corsica-Sardinia block crustal thickness is as high as 30–35 km (Figure 9b). This is confirmed by various seismic refraction and receiver function studies and gravity inversion modeling (Bethoux et al., 1999; Chamot-Rooke et al., 1999). Based upon the same types of data, crustal thickness below Sardinia is around 25 km (Gailler et al., 2009). Coverage of magnetic data in the Liguro-Provençal basin is incomplete and a clear extinct ridge is difficult to identify (Figure 9c). We tentatively interpreted one (Figures 4b and 9), primarily based on the Bouguer gravity data.

The continental crust of the Corsica-Sardinia block covers an area of ~1.11×10^5 km^2 (Table 1). Using the crustal thickness below the Corsica-Sardinia block from 0.5° resolution EPcrust model from Molinari and Morelli (2011), we calculate a total crustal volume of ~2.42×10^6 km^3 for the Corsica-Sardinia block (Table 1).

A vertical profile through the selected seismic tomographic model shows a distinct high velocity anomaly in the upper mantle below the central Mediterranean which is interpreted as the Calabrian slab (Figures 9d and S4). The slab is still connected to the surface and has a subvertical dip down toward the 660 km discontinuity on which it has draped during SE directed trench-retreat.

3.4. Microcontinents in the Scotia Sea

The Scotia Sea region, located between the Antarctic Peninsula and the southernmost tip of South America (Figures 1 and 5), contains many small basins. It is bounded by an active trench to the east, the Shackleton Fracture Zone to the west, and the North and South Scotia Ridges to the north and south. These ridges contain multiple microcontinents (see section 2.4), however we will mainly focus on the South Orkney Microcontinent and the Terror Rise and their conjugates on the Antarctic and South American margins (Figure 5). The South Orkney Microcontinent is the largest microcontinent along the South Scotia Ridge (250 × 350 km) and the Terror Rise (180 × 70 km) represents the site of the most recent breakup between Tierra del Fuego and the microcontinents along the South Scotia Ridge.

The continental nature of the various microcontinents that line the South and North Scotia Ridges is established via their seismic signature in both refraction and reflection experiments, (Bry et al., 2004; Eagles

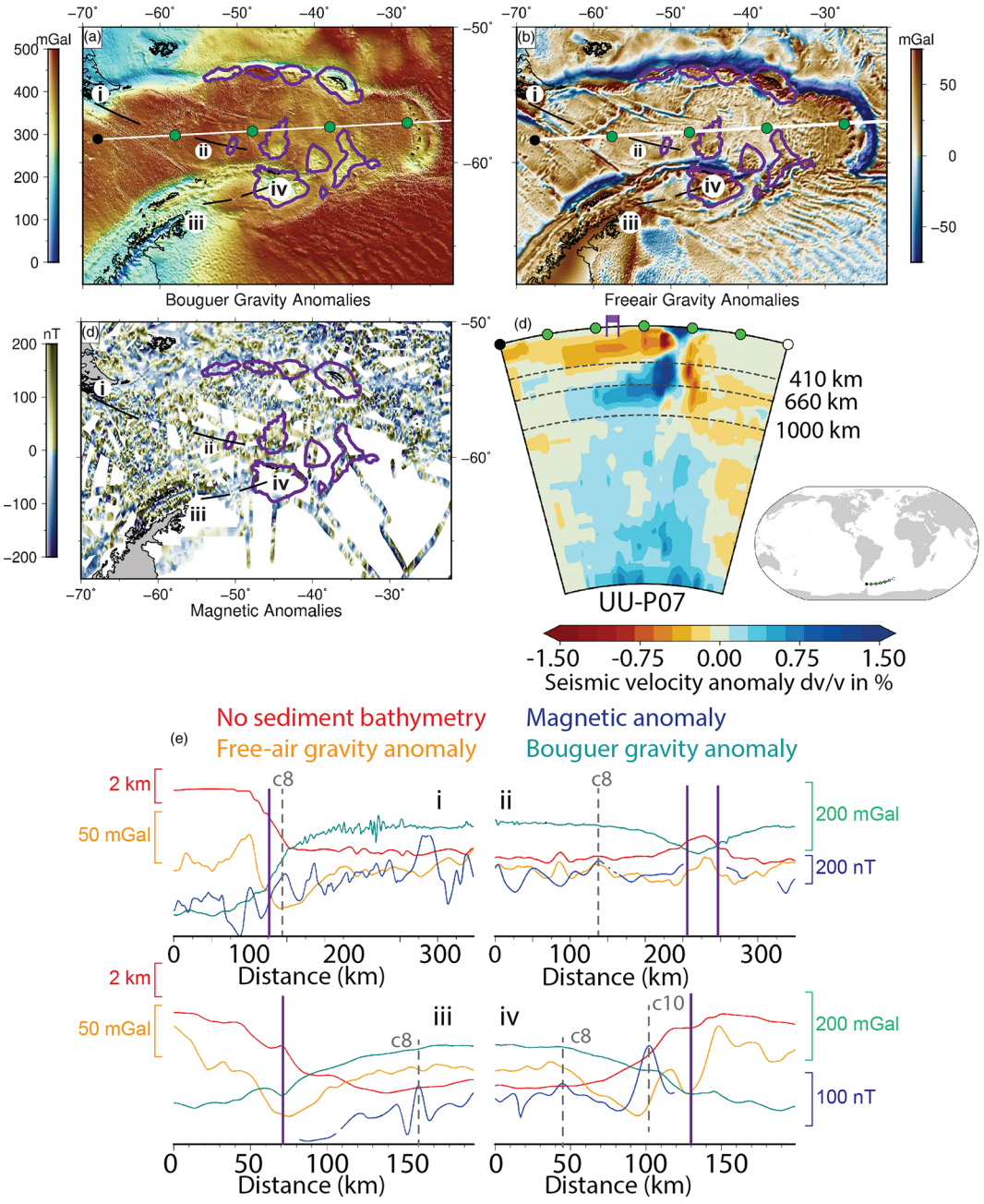

Figure 10. Geophysical data and models for the Scotia Sea region. Note the COB of the various microcontinents. Legend as in Figure 5. The white line in panels (a) and (b) represents the profile along which the tomographic section is extracted. (a) Bouguer Gravity Anomalies. (b) Free-air Gravity Anomalies. (c) Magnetic anomalies, first spreading anomalies based on Eagles and Livermore (2002) and Eagles et al. (2005). (d) Seismic tomography section from UU-P07 crossing the Scotia Sea region. (e) Profiles of geophysical data extracted along profiles i, ii, iii, and iv. See Figures 5 and 10a–10c for location (black thin lines).

et al., 2006; Pandey et al., 2010), their magnetic signature (Eagles et al., 2006), and their conjugate position to the Tierra del Fuego margin (Eagles et al., 2006; Eagles & Jokat, 2014). Outcropping continental rock on the South Georgia and South Orkney Islands (Carter et al., 2014; Dalziel et al., 1981; Trouw et al., 1997) also provide undisputable evidence for their continental nature.

As there is no published COB available, nor any indication of the COB in seismic data, we tentatively interpret the extent of the various microcontinents from potential field data (Figures 5 and 10). The lateral transforms of the North and South Scotia Ridges have strong signatures in the geophysical data, hindering the

delineation of various microcontinents (Figure 10). However, by using bathymetric data as a starting point and combining it with free air and Bouguer gravity anomalies we tentatively interpret the extent of the various microcontinents in the region.

Along the Southern Scotia Ridge, the outline of the South Orkney Microcontinent is clearly visible in all gravity and bathymetric data (Figures 5a and 10). Some of the smaller southern banks (Terror Rise, Pirie, and Jane Banks) have a less pronounced signature (Figures 5a and 10), likely due to their extended continental nature. The various sedimentary basins in between the Terror Rise, Pirie Bank, and Bruce Bank have also a distinct signature in the Bouguer gravity field (Figure 10a), aiding in the interpretation of these microcontinents.

The Terror Rise COB interpreted on the selected profile lies at ca. 100 km landward from magnetic anomaly C8 (Figure 10e). On the South American side, this distance is around 20 km. The magnetic anomalies along the South Orkney Microcontinent-Antarctica profiles have very low amplitude variations, which may show either high sediment thickness or possibly the presence of lower magnetic crust, like serpentinized exhumed mantle. Nonetheless, we interpret a distance of roughly 90 km between the Antarctic COB and the C8 anomaly and 30 km between the C10 anomaly and the South Orkney Microcontinent COB (Figure 10e).

Profiles crossing the margins of both the South American-Terror Rise and the South Orkney Microcontinent-Antarctica conjugates show a distinct difference between the two margin sets (Figure 10d). The South American margin has a clear and distinct shelf break and transition into the oceanic domain, primarily observable in the Bouguer gravity anomalies. Amplitudes of the geophysical data are much less pronounced on the Terror Rise, but as the profile crosses the entire Terror Rise, its extent is clear (Figure 10e).

Based on seismic reflection data, Coren et al. (1997) interpreted transitional crust on the two conjugate margins of the Powel basin which is about 60 km wide on the Antarctic side and approximately 20 km wide on the side of the South Orkney Microcontinent. The profiles crossing the margins of Antarctica and the South Orkney Microcontinent have much a smoother signature and the aforementioned COTs cannot be recognized (Figure 10e). The margin of the South Orkney Microcontinent appears to be slightly steeper, matching the potential asymmetry postulated above.

Seismic refraction data indicate that crustal thickness of the South Orkney Microcontinent is around 22–25 km (King & Barker, 1988). While we did not find any refraction experiments that cross the Terror Rise in the literature, we did find refraction data on its southeastern conjugate, the Pirie Bank, which has a crustal thickness of ~18 km (King & Barker, 1988). The crustal thickness beneath the Discovery bank is in the range of 23–28 km (Vuan et al., 2005) as inferred from surface wave tomography. *S* wave velocity models indicate a Moho depth of between 17 and 20 km below the South Scotia Ridge (Vuan et al., 1999). As these data are all roughly within the same range and the Terror Rise appears to be formed by extended continental crust, we assign a continental crustal thickness for this block of 17 km. Crustal thickness below thus the North Scotia Ridge is, between 16 and 19 km according to *S* wave velocity models (Vuan et al., 1999).

Using our tentative interpretations for the extent of the microcontinents in the Scotia Sea region, we find that they constitute a total area of ~2.82×10^5 km^2. Using published crustal thickness data, we ascertain a total crustal volume of microcontinents in the Scotia Sea region of ~5.57×10^6 km^3. An overview of the areas, thicknesses, and volumes of Scotia Sea microcontinents is presented in Table 1.

Seismic tomography profile across the Scotia Sea shows a thin fast anomaly extending from the surface to 410 km where it becomes wider and almost subvertical up to the 660 km discontinuity (Figure 10d). The fast anomaly seems to continue with a horizontal, wider anomaly along and below the 660 km discontinuity. Other tomographic models show either a very weak vertical fast anomaly or one that lies flat on the 660 km discontinuity (Figure S5). We interpret this fast anomaly as the subducting South American oceanic lithosphere. Faster anomalies are observed in the lower mantle, but if they are slabs, they may be connected with older episodes of subduction (Figure 10d).

3.5. Microcontinents in the Gulf of California

Originally attached to the North-American plate, the Baja California started to detach following breakup occurred in the Gulf of California (Stock & Hodges, 1989). As it is not completely separated from the North American continent (Figure 6), Baja California can be considered a proto-microcontinent.

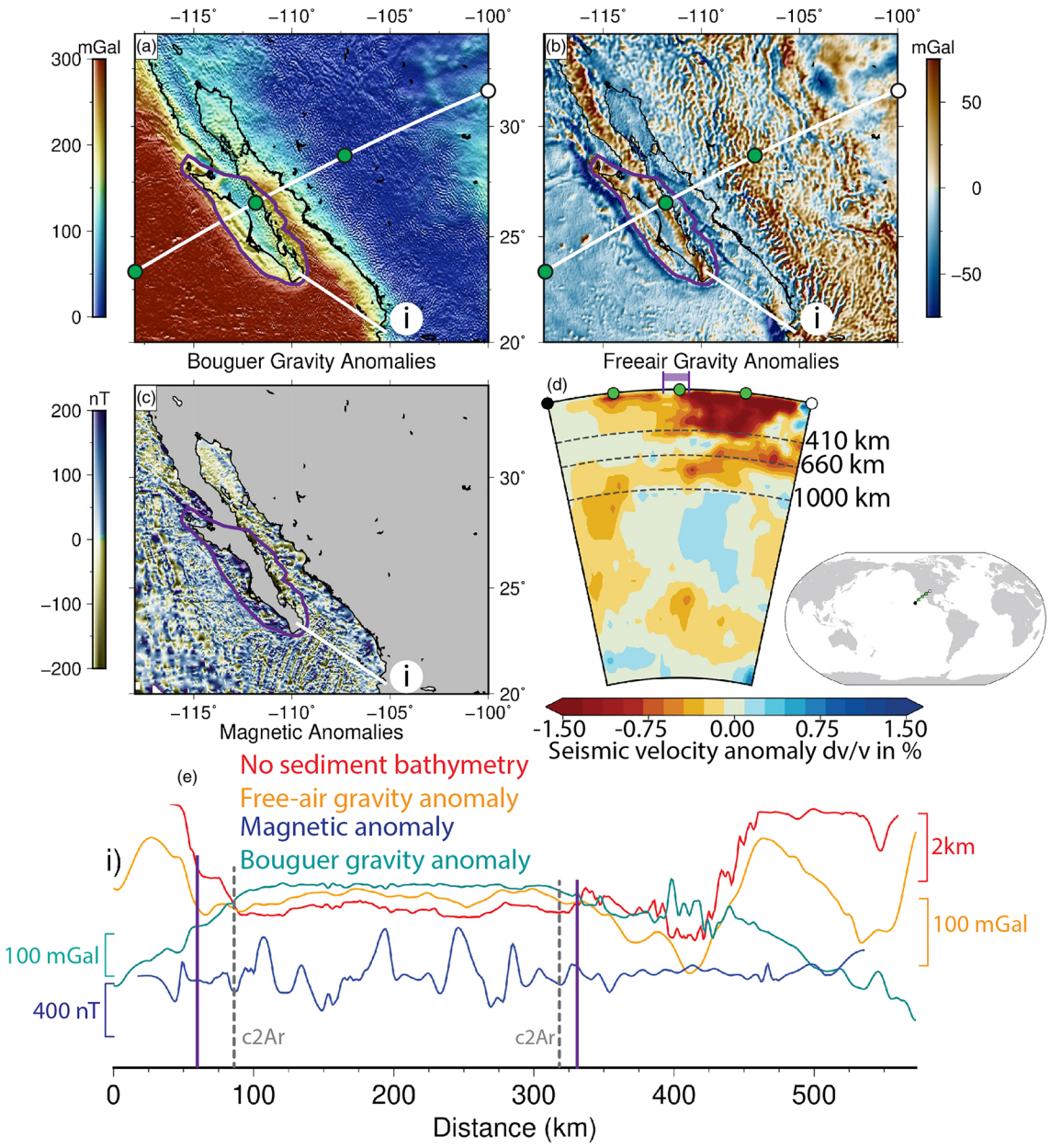

Figure 11. Geophysical data and models for the Gulf of California region. Legend as in Figure 6. The white line in panels (a) and (b) represents the profile along which the tomographic section is extracted. (a) Bouguer Gravity Anomalies. (b) Free-air Gravity Anomalies. (c) Magnetic anomalies, first spreading anomalies based on Ness et al. (1991). (d) Seismic tomography section from UU-P07 crossing the South China Sea region. (e) Section of geophysical data extracted along profile i. See Figure 6 and 11a–11c for location (black thin lines).

Separated from the Mexican mainland by the Gulf of California, Baja California is around 200 km long and its length (up to the northernmost part of Gulf of California) is approximately 1,000 km. To the west, it is bounded by the Guadalupe and Magdalena oceanic microplates, which are thought to be remnants of the Farallon plate. The continental nature of the Baja California is indicated by seismic refraction experiments and receiver function analysis (Lizarralde et al., 2007; Persaud et al., 2007).

A full set of continent ocean boundaries or transition zone location is lacking, but Sutherland et al. (2012) did interpret a COT on a seismic reflection/refraction line across the southern part of the Gulf of Mexico. Based on their interpretation, conjugate COT widths differ by about 5 km, with a 14 km wide COT on the Baja California side and a 19 km wide COT for the conjugate North-American margin (Figure 11e). Using the

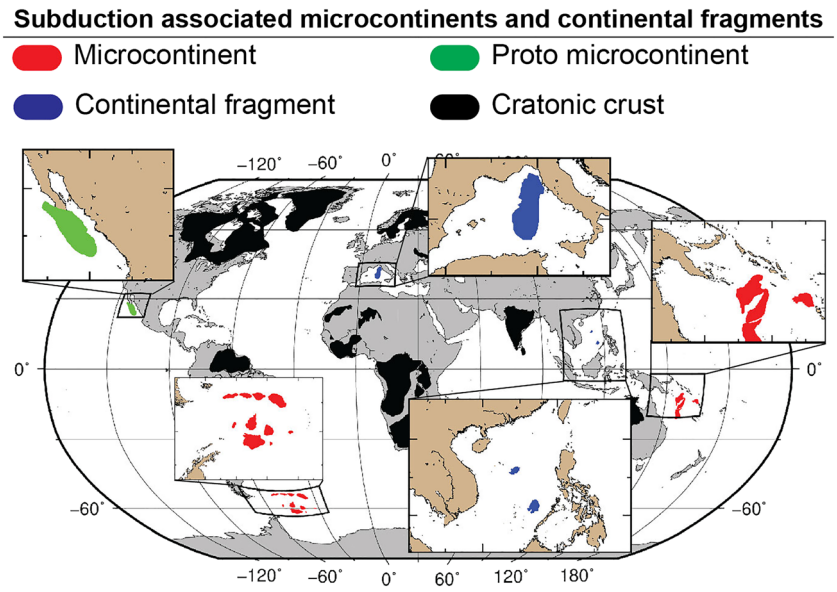

Figure 12. Overview of the extent various microcontinents and continental fragments associated with subduction systems discussed in this paper as well as the area and volume. The black area represents cratonic continental crust and is neglected in the calculations. See the text for details on area and volumetric calculations.

selected geophysical data in this study, we tentatively identify the extent of the Baja California proto-microcontinent (Figures 6a and 11). The western boundary is delineated by the paleo plate-boundary of the subduction zone. Although Baja California is still attached to the North-American continent, we interpret a northern boundary around 27.5° north which coincides with changes in the Bouguer gravity anomalies signature (Figure 11a), changes in the crustal thickness (Figure 11b), and with the northern extent of >250 mGal Bouguer gravity anomaly in the Gulf of California basin (Figure 11a).

Along the extracted profile (Figure 11e, profile i), we identify a region of roughly 50 km between the interpreted COB of Baja California and the C2Ar magnetic anomaly that could be related to oceanic spreading. On the conjugate North American side, this region is around 10 km wide (Figure 11e). Crustal thickness of the Baja California block is variable, with a 29–34 km thick crust beneath the western side of the peninsula, and a thinner 24–27 km thick crust underneath the eastern side (López-Pineda et al., 2007; Persaud et al., 2007). Crustal thickness in the conjugate North-American plate is also variable, with a thickness of 18 km in the south to 32 km in the north (López-Pineda et al., 2007).

Using the identified extent of the Baja California proto-microcontinent, we find a total area of ~1.7×10^5 km^2. A crustal volume for the Baja California proto-microcontinent of ~3.1×10^6 km^3 is calculated using crustal thickness from Crust1.0 from Laske et al. (2012).

A rather diffuse fast anomaly can be observed in the upper mantle below the Gulf of California between 410 and 660 km depth (Figures 11d and S6), and probably unlikely to be the Farallon slab. A larger, almost vertical fast anomaly is observed in the lower mantle, below 1,000 km. Previous tomographic studies suggest the Farallon plate traveled a longer distance to the east and is now located in the lower mantle (van der Meer et al., 2010).

The interaction of the subducting Farallon-Pacific active mid-ocean ridge and the continental North America led to the fragmentation of the Farallon plate in two smaller plates, the Magdalena and Guadalupe microplates, and the formation of a slab window. Recent studies based on denser seismological data were able to image these subducted microplates and the slab window in the upper mantle below the Gulf of California (Paulssen & de Vos, 2017). A high-velocity anomaly of 40 to 60 km thickness situated at depths of 115 to 135 km has been imaged below southern and central Baja California; this anomaly does not continue to the north implying the presence of a slab window. Paulssen and de Vos (2017) suggest that the subducted slab remnants cause coupling between Baja California and Pacific which influence the slow detachment of the proto-microcontinent.

4. Observed Patterns in Microcontinent Formation in Subduction Systems

In this paper we have identified and described various microcontinents that formed in (association with) subduction systems worldwide (Figure 12) where extension in the upper or lower plate is linked to the dynamics of subducted slabs and surrounding mantle. Guided by our chosen examples and previously proposed mechanisms for microcontinent formation in extensional settings, our goal is to identify possible links between the structure of preserved microcontinents, of surrounding oceanic basins, and identified subducted slabs. These causal links may give clues of how active continental margins were affected by subduction in geological time.

4.1. Potential Microcontinent Formation Mechanisms

Mechanisms that explain microcontinent formation can be roughly divided into two categories. The first category proposes that plate boundary relocations (ridge jumps) assisted by mantle heterogeneities can lead to microcontinent formation (Abera et al., 2016; Müller et al., 2001). A second category emphasizes the role of inherited tectonic structures and the need for a strike-slip motion, or a rotational component in the breakup processes resulting in the isolation of a small fragment of continental crust (Molnar et al., 2018; Nemčok et al., 2016; Péron-Pinvidic & Manatschal, 2010; van den Broek et al., 2020). The microcontinents described in this paper appear to have mainly formed via mechanisms of the second category.

4.1.1. Rotational Kinematics and Inherited Structures

All basins that separate microcontinents from their parent continents experienced a diachronous breakup and propagating mid-ocean ridges. This was caused by either rotational development of the system, such as in the Mediterranean Sea, or by oblique plate motions, such as those present in the Gulf of California. Furthermore, most of the microcontinents described here have formed in a back-arc setting with a retreating slab. The notable exception to this are the microcontinents in the South China Sea where the South China Sea basin was in a lower plate position with respect to the trench (Figure 3) (Hall & Breitfeld, 2017). Coral Sea opening could also have been triggered by a northward subducted slab, but this scenario is still debated (i.e., Whattam et al., 2008).

Another aspect that all subduction-associated microcontinents have in common is a long and complex tectonic history. The preextensional tectonic settings of all examples discussed above, except the Scotia Sea, are characterized by long-lived accretionary margins. Such margins tend to display crustal growth during their lifetime, usually resulting from the accretion of allochtonous terranes to the overriding plate (Cawood et al., 2009; Stern & Scholl, 2010; Tetreault & Buiter, 2012). The accretion or subduction of such terranes is dependent on the rheological and geometrical structure of the incoming terrane (Tetreault & Buiter, 2012), however any accreted fragments likely result in the formation of lithospheric scale inherited structures as they are transferred from the lower to the upper plate.

Recent analogue and numerical work indicates that this combination of rotational kinematics with inherited structures is a requirement for continental rifting and microcontinent formation (Molnar et al., 2018; van den Broek et al., 2020). The differential motion applied to different segments of the crust induces differential stress, which then localizes in an inherited weak zone. Formation of the Corsica-Sardinia block is likely to be the result of this kind of mechanism (van den Broek et al., 2020).

4.1.2. Hot, Thick Crust and Oblique Rifting

In addition to inherited tectonic structures, the initial thermal configuration of the crust can also play an important role in the evolution of rifting. The increasing temperatures result in decreased crust-mantle coupling, profoundly influencing margin evolution (Brune et al., 2017). However, as different initial configurations can yield similar results, it is difficult to draw any conclusions about the preextension configuration based on the final rift architecture (Brune et al., 2017).

Both the South China Sea and the Gulf of California where characterized by long-lived accretionary margins that likely resulted in a hot and thick crust in the preextensional overriding plate. Both regions also experienced rifting over large areas before strain localization resulted in continental breakup and oceanic basin formation. Finally, both regions show a distinct slow velocity anomaly in the upper mantle (Figures 8 and 11). A similar situation might have occurred in the Coral Sea, but we lack data to make any further inferences.

Formation of (proto-)microcontinents in the South China Sea and the Gulf of California suggest that hot and thick convergent margins that have a heterogeneous architecture are prime locations for microcontinent formation in a subduction setting. While the exact mechanism responsible for formation of the microcontinents in the South China Sea remains enigmatic at this time, the Gulf of California provides some more clues.

In the Gulf of California, continental breakup occurred after detachment of an oceanic slab, possibly formed by the fragmentation of the Farallon slab. However, as evidenced by the Mexican Basin and Range province, the North-American upper plate was already experiencing (back-arc) extension prior to the oceanic slab breakoff (Ferrari et al., 2018). As the subducting slab was very young, it may have subducted with a shallow dip. This shallow slab dip likely inhibited the formation of a back-arc basin that requires steeper slabs with a dip greater than 50° (Lallemand et al., 2005).

Present-day spreading in the Gulf of California is also highly oblique (Figures 6 and 11), likely related to the highly diachronous subduction of the oceanic plate. Furthermore, results from numerical modeling indicate that oblique rifting is energetically favorable to continental breakup (Brune et al., 2012). We thus speculate that the oceanic slab breakoff may have altered the stress state of the upper plate enhancing the breakup started by the highly oblique propagation of the mid-ocean ridge into North American continent.

4.1.3. Continental Crust Fragmentation

We are missing a clear mechanism explaining the formation of microcontinents in the Coral and Scotia Sea regions. Both regions show some interesting similarities: (1) a high number of smaller scattered continental blocks (Table S1/Figure 7), and (2) a location at the junction between large tectonic plates.

The Scotia Sea region is sandwiched between the South American and Antarctic plates whereas the Coral Sea was close to the interaction of the Australian, Pacific, and Eurasian plates (Figures 2 and 5). Such large plates are strong and long lived. Modeling of global mantle convection suggests that their size is controlled by large-scale mantle flow patterns and their lifespan is related to the reorganization of mantle flow (Mallard et al., 2016). These authors suggest that the fragmentation in smaller plates is driven by subduction geometry (Mallard et al., 2016). Indeed, the cessation of spreading in the Coral Sea has previously been related to changes in absolute plate motion vectors (Schellart et al., 2006). We thus speculate that the episodes of crust fragmentation and the formation of microcontinents in the Scotia and Coral sea regions are likely related to (larger) changes in the subduction system at the junction of large tectonic plates.

Microcontinents and continental fragment formed in active margin settings may also have played an important role in the tectonic evolution of the margins studied here. Observations on geophysical data collected from the eastern segment of the South Scotia Ridge suggests that, due to its weaker nature, continental crust localizes deformation (Galindo-Zaldívar et al., 2002). Dynamic subduction systems induce rapid changes in the stress field. The deformation of continental material would then accommodate these changes, showing the importance of microcontinents or continental fragments in subduction systems and shaping the active margins.

4.2. Rapid Microcontinent Formation

The duration of rifting/seafloor spreading connected to various microcontinents in subduction settings may also indicate a link to the subduction dynamics. Rifting between Eurasia and the Corsica-Sardinia block lasted only 9 Myr and seafloor spreading lasted around 8 Myr (Gattacceca et al., 2007; Jolivet & Faccenna, 2000). In the Scotia Sea, rifting in between the Discovery and Pirie banks and between the Pirie Bank and Terror Rise lasted 20 Myr altogether (Eagles & Jokat, 2014) (Table 1).

On the other hand, rifting in the Coral Sea region is thought to have taken 50 Myr (Bulois et al., 2018), whereas rifting in the South China Sea region took around 30 Myr (Franke et al., 2014). Seafloor spreading in these regions lasted 8 and 18 Myr, respectively (Table S1). The Gulf of California experienced a 28 Myr long rifting episode preceding breakup (Ferrari et al., 2018) (Table S1).

From these comparisons it follows that microcontinents formed in the short-lived rift and drift systems tend to be surrounded by, or are in proximity of, larger continental masses. They are, in a sense, formed in a more confined setting. Longer lived microcontinent formation tends to occur in (relatively) unconfined systems which are bounded on one side by (large) subducting oceanic plates (e.g., the South China Sea and the Coral Sea).

The formation of microcontinents in unconfined subduction systems might have longer rifting episodes as changes in subduction dynamics might be more easily accommodated in the neighboring oceanic domain without affecting too much the of the continental margins. Conversely, microcontinent formation in a confined system has shorter rift and spreading episodes. The proximity of such (large volumes of) buoyant continental material could result in limited space, which combined with dynamically changing subduction forces, induce rapid continental rifting, and microcontinent formation.

All microcontinents presented in this study formed during Cenozoic time and, to our knowledge, no Mesozoic or older subduction associated microcontinents are preserved in situ. This suggests that microcontinents formed in subduction settings have a relatively short life span. It seems likely that this is due to the fact that these microcontinents can be easily incorporated into orogenic and accretionary systems during subsequent basin closure. As such it follows that many subduction associated microcontinents are to be found in the geological record although subsequent deformation and metamorphism might complicate their recognition as such.

This observation of rapid formation and short lifespans is in agreement with recent work described by Mallard et al. (2016). These authors suggest that small plates can rapidly adjust to changes in subduction systems and that they form in tens of millions of years. Note that their 3-D modeling of mantle convection results in tectonic-plate like upper lid configuration and plate boundary dynamics, but no continental domains. However, numerical modeling and our observations may suggest that events of microcontinent formation in subduction settings can be potentially used as a proxy for identifying episodes of dynamic changes in subduction systems.

4.3. A Relation Between Microcontinent Formation Time and COT Width?

Regions of transitional or unconstrained crustal nature between the identified COB and the first magnetic anomaly associated with seafloor spreading vary between 10 (Gulf of California margin) and 150 km (margin of the Gulf of Lyon), but averaging around 50–75 km (Figures 7–11, S1, Table S1). The existence of transitional crust along these margins as well as the absence of clear syn-breakup volcanic eruptions and Seward Dipping Reflectors (SDRs) suggests that all discussed microcontinents probably formed in a magma-poor rifted margin setting.

The widest of these interpreted areas of transitional crust are located along the Terror Rise margin in the Scotia Sea region (100 km wide) and along the margin of the Gulf of Lyon in the central Mediterranean (150 km wide). Widths of this transitional crust in the more unconfined regions are generally around 50–75 km (Table S1). Microcontinents formed in the confined settings thus have wider zones of transitional crust when compared with microcontinents formed in unconfined settings. The wider regions of transitional crust in the confined settings might be the result of a low magma supply as also observed in passive margins studies (i.e., Buck, 2004), which in the cases analyzed here is pointing to a stalled or very slow subduction regime.

5. Microcontinents and Global Continental Crust Evolution

Throughout geological history microcontinents and continental ribbons played a crucial role in transferring continental crust across oceans and contributing to large continental mass formation. For example, Oaxaquia was a Proterozoic microcontinent that accreted to North America during the late Paleozoic (Ortega-Gutierrez et al., 1995). A myriad of "continental ribbons" originated from northern Gondwana and accreted to Eurasia during closure of the Paleo- and Neo-Tethys, forming the Variscan and Alpine collisional orogens (von Raumer et al., 2003). From present-day area extent of known continental crust area, ca. 14% represent old cratonic area (according to the World Geological Map published by Bouysse, 2014) (Table 1, Figure S11). The remaining crust was formed in oceanic domains as island arcs and microcontinents.

The microcontinents discussed in this paper are situated offshore and are (partially) submerged, therefore they can be easily neglected when assessing the global volume of continental crust. A first order quantification of the area and volume of these tectonic blocks shows that an area of 9.19×10^5 km^2 and a total crustal volume of 1.64×10^7 km^3 (see Table 1 for details) have formed due to subduction-related continental breakup. This is about 0.56% of the global non-cratonic continental crustal area and 0.28% of the global

non-cratonic continental crustal volume; values that can be higher as many other submerged, continental pieces in SW Pacific may be considered in the subduction-related microcontinent category.

If we add to this calculation the area and volume of in-situ preserved microcontinents associated with passive margin formation (i.e., Gaina & Whittaker, 2020) (Table 1, Figure S11), we conclude that about 2.5% of present-day extent of non-cratonic continental crust (and 1.15% of its volume) is found away from the main continental masses. While 2.5% seems low, results from 3-D mantle convection numerical models suggests that fragmentation of tectonic plates may have decreased through the geological time due to Earth's cooling (Mallard et al. 2016). This seems reasonable as the present-day age and structure of continental crust is heterogeneous. We therefore conclude that the formation of microcontinents as inferred from preserved present-day examples may have been important in the crustal formation and redistribution process in the deep time.

6. Conclusions

This study reviewed various in-situ microcontinents that formed in active continental margin settings. Our examples show that microcontinents and continental fragments affiliated with subduction settings occur worldwide. They tend to form in regions with a complex tectonic history, are often associated with back-arc regions, and are frequently bordered by small marginal basins. Their total area covers ca 9.19×10^5 km^2 although individual microcontinents or continental fragments are generally small ($<17 \times 10^4$ km^2). The active margins from which they detach often contain inherited structures. Reactivation of these structures appears to be a major factor in the formation of microcontinents and continental fragments.

We identify various common characteristics that may point to their potential formation mechanisms. Some microcontinents form in a rotational kinematic setting, while others form in an obliquely rifting setting, and both types require the presence inherited structures. Finally, formation mechanisms for the systems with multiple microcontinents are difficult to identify, but multiple plate boundary relocations within the margins of larger continental masses may be explained by the weakness of continental crust that is preferentially exploited when changes in plate motions and therefore stress redistribution occur.

Rifting and subsequent seafloor spreading in confined basins, located in close proximity of large continental masses (e.g., the Mediterranean Sea), tends to be reduced when compared to back-arc basins that form next to larger oceanic basins (e.g., the Coral Sea). We speculate that this discrepancy stems from different responses to changes in subduction dynamics.

Although differences in formation time exist, their formation is generally quick. Furthermore, all discussed subduction associated microcontinents and continental fragments have formed in the Cenozoic and no older microcontinents or continental fragments associated with active margins can be found in situ today. This is in agreement with modeling results that suggest that small subduction systems can rapidly adjust to dynamic changes. We thus suggest that formation of microcontinents in subduction systems can be used as a proxy for such changes to subduction dynamics.

Acknowledgments

We thank the Editor, the Associate Editor, an anonymous reviewer, and Alexander Cruden for their constructive reviews. Their excellent comments and suggestions substantially improved our manuscript. Both authors acknowledge support from the Research Council of Norway through its Centers of Excellence funding scheme, project 223272. They also acknowledge funding from the Horizon2020 Marie Sklodowska Curie Initial Training Network grant 674899—SUBITOP. Maps in Figures 1–12 were made using Generic Mapping Tools (GMT; Wessel et al., 2013). We have used the free application GPlates (gplates.org) for tectonic reconstructions. Seismic tomography section was constructed using the SubMachine web application (Hosseini et al., 2018). In order to avoid distortion of data we utilized perceptually uniform color schemes (Crameri, 2018a, 2018b).

References

Abera, R., van Wijk, J., & Axen, G. (2016). Formation of continental fragments: The Tamayo Bank, Gulf of California, Mexico. *Geology*, *44*(8), 595–598. https://doi.org/10.1130/G38123.1

Advokaat, E. L., van Hinsbergen, D. J. J., Maffione, M., Langereis, C. G., Vissers, R. L. M., Cherchi, A., et al. (2014). Eocene rotation of Sardinia, and the paleogeography of the western Mediterranean region. *Earth and Planetary Science Letters*, *401*, 183–195. https://doi.org/10.1016/j.epsl.2014.06.012

Amante, C., & Eakins, B. W. (2009). ETOPO1 arc-minute global relief model: Procedures. *NESDIS NGDC-24*, *NOAA Technical Memorandum*, Boulder, CO: NOAA.

Amaru, M. L. (2007). *Global travel time tomography with 3-D reference models* (Vol. 274). Utrecht, The Netherlands: Utrecht University.

Atwater, T., & Severinghaus, J. (1989, January 1). Tectonic maps of the Northeast Pacific. In Winterer, Hussong, & Decker (Eds.). The Eastern Pacific Ocean and Hawaii.

Atwater, T. (1970). Implications of plate tectonics for the Cenozoic tectonic evolution of Western North America. *GSA Bulletin*, *81*(12), 3513–3536. https://doi.org/10.1130/0016-7606(1970)81[3513:IOPTFT]2.0.CO;2

Bache, F., Olivet, J. L., Gorini, C., Aslanian, D., Labails, C., & Rabineau, M. (2010). Evolution of rifted continental margins: The case of the Gulf of Lions (Western Mediterranean Basin). *Earth and Planetary Science Letters*, *292*(3–4), 345–356. https://doi.org/10.1016/j.epsl.2010.02.001

Bai, Y., Wu, S., Liu, Z., Müller, R., Williams, S., Zahirovic, S., & Dong, D. (2015). Full-fit reconstruction of the South China Sea conjugate margins. *Tectonophysics*, *661*, 121–135. https://doi.org/10.1016/j.tecto.2015.08.028

Balmino, G., Vales, N., Bonvalot, S., & Briais, A. (2012). Spherical harmonic modelling to ultra-high degree of Bouguer and isostatic anomalies. *Journal of Geodesy*, *86*(7), 499–520. https://doi.org/10.1007/s00190-011-0533-4

Barckhausen, U., & Roeser, H. A. (2004). Seafloor Spreading Anomalies in the South China Sea Revisited. In P. Clift W. Kuhnt P. Wang & D. Hayes (Eds.), *Continent-Ocean Interactions Within East Asian Marginal Seas*, *Geophysical Monograph Series* (Vol. 149, pp. 121–125). Washington, DC: AGU.

Barker, P. (1995). Tectonic framework of the East Scotia Sea. In B Taylor (Ed.), *Backarc basins: Tectonics and magmatism* (pp. 281–314). New York, NY: Plenum. https://doi.org/10.1007/978-1-4615-1843-3_7

Barker, P., Dalziel, I. W. D., & Storey, B. C. (1991). Tectonic development of the Scotia arc region. *The geology of Antarctica* (215–248). Oxford, UK: Clarendon.

Barker, P., Lawver, L., & Larter, R. (2013). Heat-flow determinations of basement age in small oceanic basins of the southern central Scotia Sea. *Geological Society, London, Special Publications*, *381*(1), 139–150. https://doi.org/10.1144/SP381.3

Bethoux, N., Bertrand, E., Contrucci, I., Sosson, M., & Ferrandini, J. (1999). The deep structure of Corsica as inferred by a broad band seismological profile. *Geophysical Research Letters*, *26*(17), 2661–2664. https://doi.org/10.1029/1999GL005360

Bonvalot, S., Balmino, G., Briais, A., Kuhn, M., Peyrefitte, A., Vales, N., et al. (2012). World gravity map. In *Bureau Gravimetrique International (BGI), Map, CGMW-BGI-CNES728*. Paris: IRD.

Bouysse, P. (2014). *Geological Map of the World at 1: 35 000 000* (3rd ed.). Paris: CCGM.

Breitfeld, H., Hall, R., Galin, T., Forster, M., & BouDagher-Fadel, M. (2017). A Triassic to Cretaceous Sundaland–Pacific subduction margin in West Sarawak, Borneo. *Tectonophysics*, *694*, 35–56. https://doi.org/10.1016/j.tecto.2016.11.034

Brown, B., Gaina, C., & Müller, D. (2006). Circum-Antarctic palaeobathymetry: Illustrated examples from Cenozoic to recent times. *Palaeogeography, Palaeoclimatology, Palaeoecology*, *231*(1-2), 158–168. https://doi.org/10.1016/j.palaeo.2005.07.033

Brune, S., Heine, C., Clift, P., & Pérez-Gussinyé, M. (2017). Rifted margin architecture and crustal rheology: Reviewing Iberia-Newfoundland, central South Atlantic, and South China Sea. *Marine and Petroleum Geology*, *79*, 257–281. https://doi.org/10.1016/j.marpetgeo.2016.10.018

Brune, S., Popov, A., & Sobolev, S. (2012). Modeling suggests that oblique extension facilitates rifting and continental break-up. *Journal of Geophysical Research*, *117*, B08402. https://doi.org/10.1029/2011JB008860

Bry, M., White, N., Singh, S., England, R., & Trowell, C. (2004). Anatomy and formation of oblique continental collision: South Falkland basin. *Tectonics*, *23*, TC4011. https://doi.org/10.1029/2002TC001482

Buck, W. (2004). Consequences of asthenospheric variability on continental rifting. In Karner, G. D. Taylor, B. Driscoll, N. W. & Kohlstedt, D. L. (Eds.), *Rheology and Deformation of the Lithosphere at Continental Margins* (Vol. 62, pp. 1–30). New York, NY: Columbia University Press.

Bulois, C., Pubellier, M., Chamot-Rooke, N., & Delescluse, M. (2018). Successive rifting events in marginal basins: The example of the Coral Sea region (Papua New Guinea). *Tectonics*, *37*, 3–29. https://doi.org/10.1002/2017TC004783

Capitanio, F., Morra, G., & Goes, S. (2007). Dynamic models of downgoing plate-buoyancy driven subduction: Subduction motions and energy dissipation. *Earth and Planetary Science Letters*, *262*(1–2), 284–297. https://doi.org/10.1016/j.epsl.2007.07.039

Carter, A., Curtis, M., & Schwanethal, J. (2014). Cenozoic tectonic history of the South Georgia microcontinent and potential as a barrier to Pacific-Atlantic through flow. *Geology*, *42*(4), 299–302. https://doi.org/10.1130/G35091.1

Cawood, P., Kröner, A., Collins, W., Kusky, T., Mooney, W., & Windley, B. (2009). Accretionary orogens through Earth history. *Geological Society, London, Special Publications*, *318*(1), 1–36. https://doi.org/10.1144/SP318.1

Chamot-Rooke, N., Gaulier, J., & Jestin, F. (1999). Constraints on Moho depth and crustal thickness in the Liguro-Provençal basin from a 3D gravity inversion: Geodynamic implications. *Geological Society, London, Special Publications*, *156*(1), 37–61. https://doi.org/10.1144/GSL.SP.1999.156.01.04

Contrucci, I., Nercessian, A., Béthoux, N., Mauffret, A., & Pascal, G. (2001). A Ligurian (Western Mediterranean Sea) geophysical transect revisited. *Geophysical Journal International*, *146*(1), 74–97. https://doi.org/10.1046/j.0956-540X.2001.01418.x

Coren, F., Ceccone, G., Lodolo, E., Zanolla, C., Zitellini, N., Bonazzi, C., & Centonze, G. (1997). Morphology, seismic structure and tectonic development of the Powell Basin, Antarctica. *Journal of the Geological Society*, *154*(5), 849–862. https://doi.org/10.1144/gsjgs.154.5.0849

Crameri, F. (2018a). Geodynamic diagnostics, scientific visualisation and StagLab 3.0. *Geoscientific Model Development*, *11*(6), 2541–2562. https://doi.org/10.5194/gmd-11-2541-2018

Crameri, F. (2018b). *Scientific colour-maps*. Retrieved from https://doi.org/10.5281/zenodo.1243862

Cullen, A., Reemst, P., Henstra, G., Gozzard, S., & Ray, A. (2010). Rifting of the South China Sea: New perspectives. *Petroleum Geoscience*, *16*(3), 273–282. https://doi.org/10.1144/1354-079309-908

Dalziel, I., Elliot, D., Jones, D., Thomson, J., Thomson, M., Wells, N., & Zinsmeister, W. (1981). The geological significance of some Triassic microfossils from the South Orkney Islands, Scotia Ridge. *Geological Magazine*, *118*(1), 15–25. https://doi.org/10.1017/S0016756800024766

Dalziel, I., Lawver, L., Norton, I., & Gahagan, L. (2013). The Scotia Arc: Genesis, evolution, global significance. *Annual Review of Earth and Planetary Sciences*, *41*(1), 767–793. https://doi.org/10.1146/annurev-earth-050212-124155

Dewey, J., & Sengör, A. (1979). Aegean and surrounding regions: Complex multiplate and continuum tectonics in a convergent zone. *Geological Society of America Bulletin*, *90*(1), 84–92. https://doi.org/10.1130/0016-7606(1979)90<84:AASRCM>2.0.CO;2

di Rosa, M., de Giorgi, A., Marroni, M., & Vidal, O. (2017). Syn-convergence exhumation of continental crust: Evidence from structural and metamorphic analysis of the Monte Cecu area, Alpine Corsica (northern Corsica, France). *Geological Journal*, *52*(6), 919–937. https://doi.org/10.1002/gj.2857

Ding, W., Li, J., & Clift, P. (2016). Spreading dynamics and sedimentary process of the southwest sub-basin, South China Sea: Constraints from multi-channel seismic data and IODP Expedition 349. *Journal of Asian Earth Sciences*, *115*, 97–113. https://doi.org/10.1016/j.jseaes.2015.09.013

Eagles, G. (2010a). South Georgia and Gondwana's Pacific Margin: Lost in translation? *Journal of South American Earth Sciences*, *30*(2), 65–70. https://doi.org/10.1016/j.jsames.2010.04.004

Eagles, G. (2010b). The age and origin of the central Scotia Sea. *Geophysical Journal International*, *183*(2), 587–600. https://doi.org/10.1111/j.1365-246X.2010.04781.x

Eagles, G., Gohl, K., & Larter, R. (2004). High-resolution animated tectonic reconstruction of the South Pacific and West Antarctic Margin. *Geochemistry, Geophysics, Geosystems*, *5*, Q07002. https://doi.org/10.1029/2003GC000657

Eagles, G., & Jokat, W. (2014). Tectonic reconstructions for paleobathymetry in Drake Passage. *Tectonophysics*, *611*, 28–50. https://doi.org/10.1016/j.tecto.2013.11.021

Eagles, G., & Livermore, R. (2002). Opening history of Powell Basin, Antarctic Peninsula. *Marine Geology*, *185*(3-4), 195–205. https://doi.org/10.1016/S0025-3227(02)00191-3

Eagles, G., Livermore, R., Fairhead, J., & Morris, P. (2005). Tectonic evolution of the west Scotia Sea. *Journal of Geophysical Research*, *110*, B02401. https://doi.org/10.1029/2004JB003154

Eagles, G., Livermore, R., & Morris, P. (2006). Small basins in the Scotia Sea: The Eocene Drake Passage gateway. *Earth and Planetary Science Letters*, *242*(3-4), 343–353. https://doi.org/10.1016/j.epsl.2005.11.060

Eagles, G., Pérez-Díaz, L., & Scarselli, N. (2015). Getting over continent ocean boundaries. *Earth-Science Reviews*, *151*, 244–265. https://doi.org/10.1016/j.earscirev.2015.10.009

Ewing, M., Hawkins, L., & Ludwig, W. (1970). Crustal structure of the Coral Sea. *Journal of Geophysical Research*, *75*(11), 1953–1962. https://doi.org/10.1029/JB075i011p01953

Faccenna, C., Becker, T., Lucente, F., Jolivet, L., & Rossetti, F. (2001). History of subduction and back-arc extension in the Central Mediterranean. *Geophysical Journal International*, *145*(3), 809–820. https://doi.org/10.1046/j.0956-540x.2001.01435.x

Faccenna, C., Funiciello, F., Giardini, D., & Lucente, P. (2001). Episodic back-arc extension during restricted mantle convection in the Central Mediterranean. *Earth and Planetary Science Letters*, *187*(1–2), 105–116. https://doi.org/10.1016/S0012-821X(01)00280-1

Faccenna, C., Mattei, M., Funiciello, R., & Jolivet, L. (1997). Styles of back-arc extension in the Central Mediterranean. *Terra Nova*, *9*(3), 126–130. https://doi.org/10.1046/j.1365-3121.1997.d01-12.x

Faccenna, C., Piromallo, C., Crespo-blanc, A., & Jolivet, L. (2004). Lateral slab deformation and the origin of the western Mediterranean arcs. *Tectonics*, *23*(1). https://doi.org/10.1029/2002TC001488

Feary, D., Champion, D., Bultitude, R., & Davies, P. (1993). 37 Igneous and metasedimentary basement lithofacies of the Queensland plateau (Sites 824 and 825). In *Proceedings of the Ocean Drilling Program Drilling Program Scientific Results* (Vol. 133, pp. 535–540). College Station, TX.

Ferrari, L., Orozco-Esquivel, T., Bryan, S., López-Martínez, M., & Silva-Fragoso, A. (2018). Cenozoic magmatism and extension in western Mexico: Linking the Sierra Madre Occidental silicic large igneous province and the Comondú Group with the Gulf of California rift. *Earth-Science Reviews*, *183*(April), 115–152. https://doi.org/10.1016/j.earscirev.2017.04.006

Franke, D., Barckhausen, U., Baristeas, N., Engels, M., Ladage, S., Lutz, R., et al. (2011). The continent-ocean transition at the southeastern margin of the South China Sea. *Marine and Petroleum Geology*, *28*(6), 1187–1204. https://doi.org/10.1016/j.marpetgeo.2011.01.004

Franke, D., Savva, D., Pubellier, M., Steuer, S., Mouly, B., Auxietre, J.-L., et al. (2014). The final rifting evolution in the South China Sea. *Marine and Petroleum Geology*, *58*, 704–720. https://doi.org/10.1016/j.marpetgeo.2013.11.020

Gaherty, J. B., & Hager, B. H. (1994). Compositional vs. thermal buoyancy and the evolution of subducted lithosphere. *Geophysical Research Letters*, *21*(2), 141–144. https://doi.org/10.1029/93GL03466

Gailler, A., Klingelhoefer, F., Olivet, J.-L., & Aslanian, D. (2009). Crustal structure of a young margin pair: New results across the Liguro-Provencal Basin from wide-angle seismic tomography. *Earth and Planetary Science Letters*, *286*(1–2), 333–345. https://doi.org/10.1016/j.epsl.2009.07.001

Gaina, C., Gernigon, L., & Ball, P. (2009). Palaeocene-Recent plate boundaries in the NE Atlantic and the formation of the Jan Mayen microcontinent. *Journal of the Geological Society*, *166*(4), 601–616. https://doi.org/10.1144/0016-76492008-112

Gaina, C., Müller, R. D., Royer, J.-Y., & Symonds, P. (1999). Evolution of the Louisiade triple junction. *Journal of Geophysical Research*, *104*(B6), 12927–12939. https://doi.org/10.1029/1999JB900038

Gaina, C., Torsvik, T. H., van Hinsbergen, D. J. J., Medvedev, S., Werner, S. C., & Labails, C. (2013). The African plate: A history of oceanic crust accretion and subduction since the Jurassic. *Tectonophysics*, *604*, 4–25. https://doi.org/10.1016/j.tecto.2013.05.037

Gaina, J. M., & Whittaker, C. (2020). Microcontinents. In H. K. Gupta (Ed.), *Encyclopedia of Solid Earth Geophysics*, Berlin: Springer International Publishing.

Galindo-Zaldívar, J., Balanyá, J. C., Bohoyo, F., Jabaloy, A., Maldonado, A., Martínez-Martínez, J. M., et al. (2002). Active crustal fragmentation along the Scotia–Antarctic plate boundary east of the South Orkney Microcontinent (Antarctica). *Earth and Planetary Science Letters*, *204*(1-2), 33–46. https://doi.org/10.1016/S0012-821X(02)00959-7

Ganerød, M., Torsvik, T. H., van Hinsbergen, D. J. J., Gaina, C., Corfu, F., Werner, S., et al. (2011). Palaeoposition of the Seychelles microcontinent in relation to the Deccan Traps and the Plume Generation Zone in late Cretaceous-early Palaeogene time. *Geological Society, London, Special Publications*, *357*(1), 229–252. https://doi.org/10.1144/SP357.12

Gattacceca, J., Deino, A., Rizzo, R., Jones, D. S., Henry, B., Beaudoin, B., & Vadeboin, F. (2007). Miocene rotation of Sardinia: New paleomagnetic and geochronological constraints and geodynamic implications. *Earth and Planetary Science Letters*, *258*(3–4), 359–377. https://doi.org/10.1016/j.epsl.2007.02.003

Glen, R. A. (2005). The Tasmanides of eastern Australia. *Special Publication-Geological Society of London*, *246*(1), 23–96. https://doi.org/10.1144/GSL.SP.2005.246.01.02

Goes, S., Capitanio, F. A., & Morra, G. (2008). Evidence of lower-mantle slab penetration phases in plate motions. *Nature*, *451*(7181), 981–984. https://doi.org/10.1038/nature06691

Gueydan, F., Brun, J.-P., Phillippon, M., & Noury, M. (2017). Sequential extension as a record of Corsica Rotation during Apennines slab roll-back. *Tectonophysics*, *710-711*, 149–161. https://doi.org/10.1016/j.tecto.2016.12.028

Hall, R., & Breitfeld, H. T. (2017). Nature and demise of the Proto-South China Sea. *Bulletin. Geological Society of Malaysia*, *63*(63), 61–76. https://doi.org/10.7186/bgsm63201703

Hennig, J., Breitfeld, H. T., Hall, R., & Surya Nugraha, A. M. (2017). The Mesozoic tectono-magmatic evolution at the Paleo-Pacific subduction zone in West Borneo. *Gondwana Research*, *48*, 292–310. https://doi.org/10.1016/j.gr.2017.05.001

Hoffmann, K. L., Exon, N., Quilty, P. G., & Findlay, C. S. (2008). *Mellish Rise and adjacent deep water plateaus off northeast Australia: new evidence for continental basement from Cenozoic micropalaeontology and sedimentary geology* (pp. 317–323). Sydney: PESA Eastern Australian Basins Symposium III.

Hosseini, K., Matthews, K. J., Sigloch, K., Shephard, G. E., Domeier, M., & Tsekhmistrenko, M. (2018). SubMachine: Web-based tools for exploring seismic tomography and other models of Earth's deep interior. *Geochemistry, Geophysics, Geosystems*, *19*, 1464–1483. https://doi.org/10.1029/2018GC007431

Hosseini, K., Sigloch, K., Tsekhmistrenko, M., Zaheri, A., Nissen-Meyer, T., & Igel, H. (2019). Global mantle structure from multifrequency tomography using P, PP and P-diffracted waves. *Geophysical Journal International*, *220*(1), 96–141. https://doi.org/10.1093/gji/ggz394

Huang, H., He, E., Qiu, X., Guo, X., Fan, J., & Zhang, X. (2019). Insights about the structure and development of Zhongsha Bank in the South China Sea from integrated geophysical modelling. *International Geology Review*, *62*(7-8), 1070–1080. https://doi.org/10.1080/00206814.2019.1653798

Hutchison, C. S. (2004). Marginal basin evolution: The southern South China Sea. *Marine and Petroleum Geology*, *21*(9), 1129–1148. https://doi.org/10.1016/j.marpetgeo.2004.07.002

Jolivet, L., & Faccenna, C. (2000). Mediterranean extension and the Africa-Eurasia collision. *Tectonics*, *19*(6), 1095–1106. https://doi.org/10.1029/2000TC900018

Jolivet, L., Gorini, C., Smit, J., & Leroy, S. (2015). Continental breakup and the dynamics of rifting in back-arc basins: The Gulf of Lion margin. *Tectonics*, *34*, 662–679. https://doi.org/10.1002/2014TC003570

King, E. C., & Barker, P. F. (1988). The margins of the South Orkney microcontinent. *Journal of the Geological Society (London)*, *145*(2), 317–331. https://doi.org/10.1144/gsjgs.145.2.0317

Kudrass, H. R., Wiedicke, M., Cepek, P., Kreuzer, H., & Müller, P. (1986). Mesozoic and Cainozoic rocks dredged from the South China Sea (Reed Bank area) and Sulu Sea and their significance for plate-tectonic reconstructions. *Marine and Petroleum Geology*, *3*(1), 19–30. https://doi.org/10.1016/0264-8172(86)90053-X

Lacombe, O., & Jolivet, L. (2005). Structural and kinematic relationships between Corsica and the Pyrenees-Provence domain at the time of the Pyrenean orogeny. *Tectonics*, *24*, 1–20. https://doi.org/10.1029/2004TC001673

Laird, M. G., & Bradshaw, J. D. (2004). The break-up of a long-term relationship: The Cretaceous separation of New Zealand from Gondwana. *Gondwana Research*, *7*(1), 273–286. https://doi.org/10.1016/S1342-937X(05)70325-7

Lallemand, S., Heuret, A., & Boutelier, D. (2005). On the relationships between slab dip, back-arc stress, upper plate absolute motion, and crustal nature in subduction zones. *Geochemistry, Geophysics, Geosystems*, *6*, Q09006. https://doi.org/10.1029/2005GC000917

Laske, G., Masters, G., Ma, Z., & Pasyanos, M. (2012). *CRUST1. 0: An updated global model of the Earth's crust* (Vol. 14). Vienna: EGU General Assembly.

Li, C., van der Hilst, R. D., Engdahl, E. R., & Burdick, S. (2008). A new global model for P wave speed variations in Earth's mantle. *Geochemistry, Geophysics, Geosystems*, *9*, Q05018. https://doi.org/10.1029/2007GC001806

Li, C.-F., Xu, X., Lin, J., Sun, Z., Zhu, J., Yao, Y., et al. (2014). Ages and magnetic structures of the South China Sea constrained by deep tow magnetic surveys and IODP Expedition 349. *Geochemistry, Geophysics, Geosystems*, *15*, 4958–4983. https://doi.org/10.1002/2014GC005567

Lister, G. S., Etheridge, M. A., & Symonds, P. A. (1986). Detachment faulting and the evolution of passive continental margins. *Geology*, *14*(3), 246–250. https://doi.org/10.1130/0091-7613(1986)14<246:DFATEO>2.0.CO;2

Lizarralde, D., Axen, G. J., Brown, H. E., Fletcher, J. M., González-Fernández, A., Harding, A. J., et al. (2007). Variation in styles of rifting in the Gulf of California. *Nature*, *448*(7152), 466–469. https://doi.org/10.1038/nature06035

López-Pineda, L., Rebollar, C. J., & Quintanar, L. (2007). Crustal thickness estimates for Baja California, Sonora, and Sinaloa, Mexico, using disperse surface waves. *Journal of Geophysical Research*, *112*, B04308. https://doi.org/10.1029/2005JB003899

Lu, C., Grand, S. P., Lai, H., & Garnero, E. J. (2019). TX2019slab: A New P and S Tomography Model Incorporating Subducting Slabs. *Journal of Geophysical Research: Solid Earth*, *124*, 11,549–11,567. https://doi.org/10.1029/2019JB017448

Lus, W. Y., McDougall, I., & Davies, H. L. (2004). Age of the metamorphic sole of the Papuan Ultramafic Belt ophiolite, Papua New Guinea. *Tectonophysics*, *392*(1-4), 85–101. https://doi.org/10.1016/j.tecto.2004.04.009

Mallard, C., Coltice, N., Seton, M., Dietmar Müller, R., & Tackley, P. J. (2016). Subduction controls the distribution and fragmentation of Earth's tectonic plates. *Nature*, *535*(7610), 140–143. https://doi.org/10.1038/nature17992

Matthews, K. J., Maloney, K. T., Zahirovic, S., Williams, S. E., Seton, M., & Dietmar Müller, R. (2016). Global plate boundary evolution and kinematics since the late Paleozoic. *Global and Planetary Change*, *146*, 226–250. https://doi.org/10.1016/j.gloplacha.2016.10.002

Matthews, K. J., Williams, S. E., Whittaker, J. M., Müller, R. D., Seton, M., & Clarke, G. L. (2015). Geologic and kinematic constraints on late Cretaceous to mid Eocene plate boundaries in the southwest Pacific. *Earth-Science Reviews*, *140*, 72–107. https://doi.org/10.1016/j.earscirev.2014.10.008

Molinari, I., & Morelli, A. (2011). EPcrust: A reference crustal model for the European plate. *Geophysical Journal International*, *185*(1), 352–364. https://doi.org/10.1111/j.1365-246X.2011.04940.x

Molnar, N. E., Cruden, A. R., & Betts, P. G. (2018). Unzipping continents and the birth of microcontinents. *Geology*, 1–4. https://doi.org/10.1130/g40021.1

Müller, R. D., Gaina, C., Roest, W. R., & Hansen, D. L. (2001). A recipe for microcontinent formation. *Geology*, *29*(3), 203–206. https://doi.org/10.1130/0091-7613

Müller, R. D., Sdrolias, M., Gaina, C., & Roest, W. R. (2008). Age, spreading rates, and spreading asymmetry of the world's ocean crust. *Geochemistry, Geophysics, Geosystems*, *9*, Q04006. https://doi.org/10.1029/2007GC001743

Müller, R. D., Seton, M., Zahirovic, S., Williams, S. E., Matthews, K. J., Wright, N. M., et al. (2016). Ocean basin evolution and global-scale plate reorganization events since Pangea breakup. *Annual Review of Earth and Planetary Sciences*, *44*(1), 107–138. https://doi.org/10.1146/annurev-earth-060115-012211

Nemčok, M., Sinha, S. T., Doré, A. G., Lundin, E. R., Mascle, J., & Rybár, S. (2016). Mechanisms of microcontinent release associated with wrenching-involved continental break-up: A review. *Geological Society, London, Special Publications*, *431*(1), 323–359. https://doi.org/10.1144/SP431.14

Ness, G. E., Lyle, M. W., & Couch, R. W. (1991). Marine magnetic anomalies and oceanic crustal isochrons of the Gulf and Peninsular Province of the Californias. *American Association of Petroleum Geologists Memoir*, *47*, 47–69.

Ortega-Gutierrez, F., Ruiz, J., & Centeno-Garcia, E. (1995). Oaxaquia, a Proterozoic microcontinent accreted to North America during the late Paleozoic. *Geology*, *23*(12), 1127–1130. https://doi.org/10.1130/0091-7613(1995)023<1127:OAPMAT>2.3.CO;2

Pandey, A., Parson, L., & Milton, A. (2010). Geochemistry of the Davis and Aurora Banks: Possible implications on evolution of the North Scotia Ridge. *Marine Geology*, *268*(1-4), 106–114. https://doi.org/10.1016/j.margeo.2009.10.025

Paterson, N. R., & Reeves, C. V. (1985). Applications of gravity and magnetic surveys: The state-of-the-art in 1985. *Geophysics*, *50*(12), 2558–2594. https://doi.org/10.1190/1.1441884

Paulssen, H., & de Vos, D. (2017). Slab remnants beneath the Baja California peninsula: Seismic constraints and tectonic implications. *Tectonophysics*, *719*, 27–36. https://doi.org/10.1016/j.tecto.2016.09.021

Peron-Pinvidic, G., Gernigon, L., Gaina, C., & Ball, P. (2012a). Insights from the Jan Mayen system in the Norwegian-Greenland Sea-I. Mapping of a microcontinent. *Geophysical Journal International*, *191*(2), 413–435. https://doi.org/10.1111/j.1365-246X.2012.05623.x

Peron-Pinvidic, G., Gernigon, L., Gaina, C., & Ball, P. (2012b). Insights from the Jan Mayen system in the Norwegian-Greenland Sea-II. Architecture of a microcontinent. *Geophysical Journal International*, *191*(2), 413–435. https://doi.org/10.1111/j.1365-246X.2012.05623.x

Péron-Pinvidic, G., & Manatschal, G. (2010). From microcontinents to extensional allochthons: Witnesses of how continents rift and break apart? *Petroleum Geoscience*, *16*(3), 189–197. https://doi.org/10.1144/1354-079309-903

Persaud, P., Pérez-Campos, X., & Clayton, R. W. (2007). Crustal thickness variations in the margins of the Gulf of California from receiver functions. *Geophysical Journal International*, *170*(2), 687–699. https://doi.org/10.1111/j.1365-246X.2007.03412.x

Pichot, T., Delescluse, M., Chamot-Rooke, N., Pubellier, M., Qiu, Y., Meresse, F., et al. (2014). Deep crustal structure of the conjugate margins of the SW South China Sea from wide-angle refraction seismic data. *Marine and Petroleum Geology*, *58*, 627–643. https://doi.org/10.1016/j.marpetgeo.2013.10.008

Pubellier, M., Ego, F., Chamot-Rooke, N., & Rangin, C. (2003). The building of pericratonic mountain ranges: Structural and kinematic constraints applied to GIS-based reconstructions of SE Asia. *Bulletin de la Societe Geologique de France*, *174*(6), 561–584. https://doi.org/10.2113/174.6.561

Rollet, N., Déverchère, J., Beslier, M.-O., Guennoc, P., Réhault, J.-P., Sosson, M., & Truffert, C. (2002). Back arc extension, tectonic inheritance, and volcanism in the Ligurian Sea, Western Mediterranean. *Tectonics*, *21*(3), 6-1–6-23. https://doi.org/10.1029/2001TC900027

Rossi, P., Oggiano, G., & Cocherie, A. (2009). A restored section of the "southern Variscan realm" across the Corsica-Sardinia microcontinent. *Comptes Rendus Geoscience*, *341*(2–3), 224–238. https://doi.org/10.1016/j.crte.2008.12.005

Ruan, A.-G., Niu, X.-W., Qiu, X.-L., Li, J.-B., Wu, Z.-L., Zhao, M.-H., & Wei, X.-D. (2011). A wide angle ocean bottom seismometer experiment across Liyue Bank, the southern margin of the South China Sea. *Chinese Journal of Geophysics*, *54*(6), 1033–1044. https://doi.org/10.1002/cjg2.1682

Sandwell, D. T., Müller, R. D., Smith, W. H. F., Garcia, E., & Francis, R. (2014). New global marine gravity model from CryoSat-2 and Jason-1 reveals buried tectonic structure. *Science*, *346*(6205), 65–67. https://doi.org/10.1126/science.1258213

Schellart, W. P., Lister, G. S., & Toy, V. G. (2006). A late Cretaceous and Cenozoic reconstruction of the Southwest Pacific region: Tectonics controlled by subduction and slab rollback processes. *Earth-Science Reviews*, *76*(3–4), 191–233. https://doi.org/10.1016/j.earscirev.2006.01.002

Schmid, S. M., Kissling, E., Diehl, T., van Hinsbergen, D. J. J., & Molli, G. (2017). Ivrea mantle wedge, arc of the Western Alps, and kinematic evolution of the Alps–Apennines orogenic system. *Swiss Journal of Geosciences*, *110*(2), 581–612. https://doi.org/10.1007/s00015-016-0237-0

Scrutton, R. A. (1976). Microcontinents and their significance. In *Geodynamics: Progress and Prospects* (Vol. 5, pp. 177–189). Washington, DC: AGU.

Segev, A., Rybakov, M., & Mortimer, N. (2012). A crustal model for Zealandia and Fiji. *Geophysical Journal International*, *189*(3), 1277–1292. https://doi.org/10.1111/j.1365-246X.2012.05436.x

Séranne, M. (1999). The Gulf of Lion continental margin (NW Mediterranean) revisited by IBS: An overview. *Geological Society, London, Special Publications*, *156*(1), 15–36. https://doi.org/10.1144/gsl.sp.1999.156.01.03

Seton, M., Müller, R. D., Zahirovic, S., Gaina, C., Torsvik, T., Shephard, G., et al. (2012). Global continental and ocean basin reconstructions since 200 Ma. *Earth-Science Reviews*, *113*(3–4), 212–270. https://doi.org/10.1016/j.earscirev.2012.03.002

Seton, M., Mortimer, N., Williams, S., Quilty, P., Gans, P., Meffre, S., et al. (2016). Melanesian back-arc basin and arc development: Constraints from the eastern Coral Sea. *Gondwana Research*, *39*, 77–95. https://doi.org/10.1016/j.gr.2016.06.011

Shipboard Scientific Party (2000). Leg 184 Summary: Exploring the Asian Monsoon through Drilling in the South China Sea. In P. Wang, W. L. Prell, & P. Blum (Eds.), *Proceedings of the Ocean Drilling Program, Initial Reports* (Vol. 184, pp. 1–77). TX: ODP College Station.

Sibuet, J.-C., Yeh, Y.-C., & Lee, C.-S. (2016). Geodynamics of the South China Sea. *Tectonophysics*, *692*, 98–119. https://doi.org/10.1016/j.tecto.2016.02.022

Smalley, R., Dalziel, I. W. D., Bevis, M. G., Kendrick, E., Stamps, D. S., King, E. C., et al. (2007). Scotia arc kinematics from GPS geodesy. *Geophysical Research Letters*, *34*, L21308. https://doi.org/10.1029/2007GL031699

Stern, R. J., & Scholl, D. W. (2010). Yin and yang of continental crust creation and destruction by plate tectonic processes. *International Geology Review*, *52*(1), 1–31. https://doi.org/10.1080/00206810903332322

Stock, J. M., & Hodges, K. V. (1989). Pre-Pliocene extension around the Gulf of California and the transfer of Baja California to the Pacific Plate. *Tectonics*, *8*(1), 99–115. https://doi.org/10.1029/TC008i001p00099

Straume, E. O., Gaina, C., Medvedev, S., Hochmuth, K., Gohl, K., Whittaker, J. M., et al. (2019). GlobSed: Updated total sediment thickness in the world's oceans. *Geochemistry, Geophysics, Geosystems*, *20*, 1756–1772. https://doi.org/10.1029/2018GC008115

Sutherland, F. H., Kent, G. M., Harding, A. J., Umhoefer, P. J., Driscoll, N. W., Lizarralde, D., et al. (2012). Middle Miocene to early Pliocene oblique extension in the southern Gulf of California. *Geosphere*, *8*(4), 752–770. https://doi.org/10.1130/GES00770.1

Taylor, B., & Hayes, D. E. (1980). The tectonic evolution of the South China Basin. D. Hayes In *The Tectonic and Geologic Evolution of Southeast Asian Seas and Islands*, *Geophysical Monographs Series* (Vol. 23, (Figure 1), pp. 89–104). Washington, DC: AGU.

Taylor, B., & Hayes, D. E. (1983). Origin and history of the South China Sea basin. D. Hayes In *The Tectonic and Geologic Evolution of Southeast Asian Seas and Islands: Part 2*, *Geophysical Monograph Series* (Vol. 27, pp. 23–56). Washington, DC: AGU.

Taylor, L., & Falvey, D. (1977). Queensland Plateau and Coral Sea Basin; stratigraphy, structure and tectonics. *The APPEA Journal*, *17*(1), 13. https://doi.org/10.1071/AJ76002

Tetreault, J. L., & Buiter, S. J. H. (2012). Geodynamic models of terrane accretion: Testing the fate of island arcs, oceanic plateaus, and continental fragments in subduction zones. *Journal of Geophysical Research*, *117*, B08403. https://doi.org/10.1029/2012JB009316

Torsvik, T. H., Amundsen, H., Hartz, E. H., Corfu, F., Kusznir, N., Gaina, C., et al. (2013). A Precambrian microcontinent in the Indian Ocean. *Nature Geoscience*, *6*(3), 223–227. https://doi.org/10.1038/ngeo1736

Trouw, R. A. J., Passchier, C. W., Simões, L. S. A., Andreis, R. R., & Valeriano, C. M. (1997). Mesozoic tectonic evolution of the South Orkney Microcontinent, Scotia arc, Antarctica. *Geological Magazine*, *134*(3), 383–401. https://doi.org/10.1017/S0016756897007036

Turco, E., Macchiavelli, C., Mazzoli, S., Schettino, A., & Pierantoni, P. P. (2012). Kinematic evolution of Alpine Corsica in the framework of Mediterranean mountain belts. *Tectonophysics*, *579*, 193–206. https://doi.org/10.1016/j.tecto.2012.05.010

Umhoefer, P. J. (2011). Why did the Southern Gulf of California rupture so rapidly?—Oblique divergence across hot, weak lithosphere along a tectonically active margin. *GSA Today*, *21*(11), 4–10. https://doi.org/10.1130/G133A.1

van den Broek, J. M., Magni, V., Gaina, C., & Buiter, S. J. H. (2020). The formation of continental fragments in subduction settings: The importance of structural inheritance and subduction system dynamics. *Journal of Geophysical Research: Solid Earth*. https://doi.org/10.1029/2019JB018370

van der Meer, D. G., Spakman, W., van Hinsbergen, D. J. J., Amaru, M. L., & Torsvik, T. H. (2010). Towards absolute plate motions constrained by lower-mantle slab remnants. *Nature Geoscience*, *3*(1), 36–40. https://doi.org/10.1038/ngeo708

van Hinsbergen, D. J. J., Vissers, R. L. M., & Spakman, W. (2014). Origin and consequences of western Mediterranean subduction, rollback, and slab segmentation. *Tectonics*, *33*, 393–419. https://doi.org/10.1002/2013TC003349

Van Wyck, N., & Williams, I. S. (2002). Age and provenance of basement metasediments from the Kubor and Bena Bena Blocks, central Highlands, Papua New Guinea: Constraints on the tectonic evolution of the northern Australian cratonic margin. *Australian Journal of Earth Sciences*, *49*(3), 565–577. https://doi.org/10.1046/j.1440-0952.2002.00938.x

Vanneste, L. E., & Larter, R. D. (2002). Sediment subduction, subduction erosion, and strain regime in the northern South Sandwich forearc. *Journal of Geophysical Research*, *107*(B7), 2149. https://doi.org/10.1029/2001JB000396

Vissers, R. L. M., van Hinsbergen, D. J. J., Meijer, P. T., & Piccardo, G. B. (2013). Kinematics of Jurassic ultra-slow spreading in the Piemonte Ligurian Ocean. *Earth and Planetary Science Letters*, *380*, 138–150. https://doi.org/10.1016/j.epsl.2013.08.033

von Raumer, J. F., Stampfli, G. M., & Bussy, F. (2003). Gondwana-derived microcontinents—The constituents of the Variscan and Alpine collisional orogens. *Tectonophysics*, *365*(1–4), 7–22. https://doi.org/10.1016/S0040-1951(03)00015-5

Vuan, A., Cazzaro, R., Costa, G., Russi, M., & Panza, G. F. (1999). S-wave velocity models in the Scotia Sea region, Antarctica, from nonlinear inversion of Rayleigh waves dispersion. *Pure and Applied Geophysics*, *154*(1), 121–139. https://doi.org/10.1007/s000240050224

Vuan, A., Lodolo, E., Panza, G. F., & Sauli, C. (2005). Crustal structure beneath Discovery Bank in the Scotia Sea from group velocity tomography and seismic reflection data. *Antarctic Science*, *17*(1), 97–106. https://doi.org/10.1017/S0954102005002488

Wang, T. K., Chen, M.-K., Lee, C.-S., & Xia, K. (2006). Seismic imaging of the transitional crust across the northeastern margin of the South China Sea. *Tectonophysics*, *412*(3–4), 237–254. https://doi.org/10.1016/j.tecto.2005.10.039

Webb, L. E., Baldwin, S. L., & Fitzgerald, P. G. (2014). The Early-Middle Miocene subduction complex of the Louisiade Archipelago, southern margin of the Woodlark Rift. *Geochemistry, Geophysics, Geosystems*, *15*, 4024–4046. https://doi.org/10.1002/2014GC005500

Weissel, J. K., & Watts, A. B. (1979). Tectonic evolution of the Coral Sea Basin. *Journal of Geophysical Research*, *84*(B9), 4572–4582. https://doi.org/10.1029/JB084iB09p04572

Wessel, P., Smith, W. H. F., Scharroo, R., Luis, J., & Wobbe, F. (2013). Generic mapping tools: Improved version released. *Eos, Transactions American Geophysical Union*, *94*(45), 409–410. https://doi.org/10.1002/2013EO450001

Whattam, S. A., Malpas, J., Ali, J. R., & Smith, I. E. M. (2008). New SW Pacific tectonic model: Cyclical intraoceanic magmatic arc construction and near-coeval emplacement along the Australia-Pacific margin in the Cenozoic. *Geochemistry, Geophysics, Geosystems*, *9*, Q03021. https://doi.org/10.1029/2007GC001710

Wright, N. M., Seton, M., Williams, S. E., & Dietmar Müller, R. (2016). The late Cretaceous to recent tectonic history of the Pacific Ocean basin. *Earth-Science Reviews*, *154*, 138–173. https://doi.org/10.1016/j.earscirev.2015.11.015

Wu, J., Suppe, J., Lu, R., & Kanda, R. (2016). Philippine Sea and East Asian plate tectonics since 52 Ma constrained by new subducted slab reconstruction methods. *Journal of Geophysical Research: Solid Earth*, *121*, 4670–4741. https://doi.org/10.1002/2016JB012923

Wu, Z. L., Li, J. B., Ruan, A. G., Lou, H., Ding, W. W., Niu, X. W., & Li, X. B. (2012). Crustal structure of the northwestern sub-basin, South China Sea: Results from a wide-angle seismic experiment. *Science China Earth Sciences*, *55*(1), 159–172. https://doi.org/10.1007/s11430-011-4324-9

Yumul, G. P., Dimalanta, C. B., Tamayo, R. A., & Maury, R. C. (2003). Collision, subduction and accretion events in the Philippines: A synthesis. *The Island Arc*, *12*(2), 77–91. https://doi.org/10.1046/j.1440-1738.2003.00382.x

Zahirovic, S., Seton, M., & Müller, R. D. (2014). The Cretaceous and Cenozoic tectonic evolution of Southeast Asia. *Solid Earth*, *5*(1), 227–273. https://doi.org/10.5194/se-5-227-2014